

# Accepted Manuscript

Difuran-substituted quinoxalines as a novel class of PI3K $\alpha$  H1047R mutant inhibitors: Synthesis, biological evaluation and structure-activity relationship

Ning Zhang, Zhimei Yu, Xiaohong Yang, Yan Zhou, Qing Tang, Ping Hu, Jia Wang, Shao-Lin Zhang, Ming-Wei Wang, Yun He



PII: S0223-5234(18)30626-3

DOI: [10.1016/j.ejmech.2018.07.061](https://doi.org/10.1016/j.ejmech.2018.07.061)

Reference: EJMECH 10596

To appear in: *European Journal of Medicinal Chemistry*

Received Date: 13 May 2018

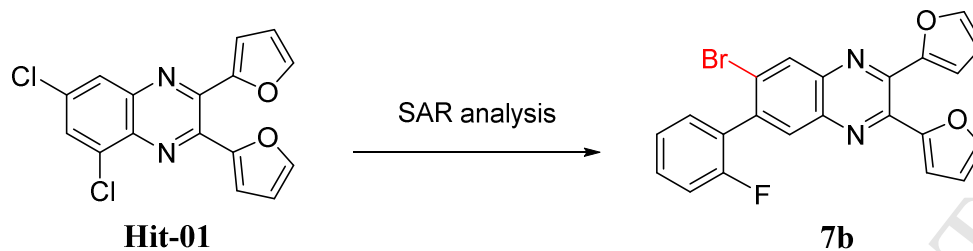
Revised Date: 25 July 2018

Accepted Date: 25 July 2018

Please cite this article as: N. Zhang, Z. Yu, X. Yang, Y. Zhou, Q. Tang, P. Hu, J. Wang, S.-L. Zhang, M.-W. Wang, Y. He, Difuran-substituted quinoxalines as a novel class of PI3K $\alpha$  H1047R mutant inhibitors: Synthesis, biological evaluation and structure-activity relationship, *European Journal of Medicinal Chemistry* (2018), doi: 10.1016/j.ejmech.2018.07.061.

This is a PDF file of an unedited manuscript that has been accepted for publication. As a service to our customers we are providing this early version of the manuscript. The manuscript will undergo copyediting, typesetting, and review of the resulting proof before it is published in its final form. Please note that during the production process errors may be discovered which could affect the content, and all legal disclaimers that apply to the journal pertain.

## Graphical Abstract



Comp.	$EC_{50}$ ( $\mu\text{M}$ )		$IC_{50}$ ( $\mu\text{M}$ )		Improved potency ( <b>Hit-01</b> to <b>7b</b> )
	PI3K $\alpha$ H1047R mutant	PI3K $\alpha$ WT	HCT116		
<b>Hit-01</b>	76.0	NT	> 100		76.0 / 0.137 > 500 (enzymatic level)
<b>7b</b>	0.137	0.093	11.2		100 / 11.2 > 9 (cellular level)

**Title:**

Difuran-substituted quinoxalines as a novel class of PI3K $\alpha$  H1047R mutant inhibitors: Synthesis, biological evaluation and structure-activity relationship

**Author names and affiliations:**

Ning Zhang<sup>1</sup>, Zhimei Yu<sup>1</sup>, Xiaohong Yang<sup>1</sup>, Yan Zhou<sup>2</sup>, Qing Tang<sup>1</sup>, Ping Hu<sup>1</sup>, Jia Wang<sup>2</sup>, Shao-Lin Zhang<sup>1\*</sup>, Ming-Wei Wang<sup>2\*</sup>, and Yun He<sup>1\*</sup>

<sup>1</sup> School of Pharmaceutical Sciences, Chongqing Key Laboratory of Natural Product Synthesis and Drug Research, Chongqing University, Chongqing, 401331, P. R. China

<sup>2</sup> The National Center for Drug Screening and the CAS Key Laboratory of Receptor Research, Shanghai Institute of Materia Medica, Chinese Academy of Sciences (CAS), 189 Guo Shou Jing Road, Shanghai, 201203, China

**\* Corresponding address:**

Tel.: +86-23-65678465; E-mail: [zhangsl@cqu.edu.cn](mailto:zhangsl@cqu.edu.cn); [mwwang@simm.ac.cn](mailto:mwwang@simm.ac.cn); [yun.he@cqu.edu.cn](mailto:yun.he@cqu.edu.cn)

**Abstract:**

Phosphatidylinositol 3-kinase  $\alpha$  (PI3K $\alpha$ ) is the most frequently mutated kinase in human cancers, making it an attractive therapeutic target for cancer treatment. We identified a structurally novel PI3K $\alpha$  H1047R mutant inhibitor **Hit-01** (EC<sub>50</sub> = 76.0  $\mu$ M) through a high-throughput screening campaign. Chemical optimizations enabled us to discover compound **7b**, which strongly inhibited PI3K $\alpha$  H1047R mutant with an EC<sub>50</sub> value of 0.137  $\mu$ M, over 500-fold more potent than **Hit-01**. Western blotting analysis suggested that **7b** could decrease the phosphorylation level of *p*-AKT, another proof that **7b** inhibited PI3K $\alpha$  H1047R function. Cell viability assay revealed that **7b** inhibited HCT116 cancer cell growth with an IC<sub>50</sub> value of 11.23  $\mu$ M. In addition, **7b** was found to arrest cell cycle at G1 phase and induce cell apoptosis *via* up-regulation of caspase-3, caspase-8 and caspase-9 protein expressions. Collectively, all these data demonstrated that **7b** could be a promising lead for the development of structurally novel PI3K $\alpha$  inhibitors.

**Keywords:**

Proliferation; Anticancer drug; Phosphatidylinositol 3-kinase inhibitor; Apoptosis;

Structure-activity relationship

ACCEPTED MANUSCRIPT

## 1. Introduction

The phosphatidylinositol-3-kinase (PI3K) signaling pathway plays key regulatory roles in multiple cellular functions including cell growth, survival, proliferation, differentiation and invasion [1-5]. The PI3Ks family could be divided into several different subtypes according their structural characteristics and substrate specificity [6-9]. Among which, the PI3K $\alpha$  is frequently activated, amplified and mutated in human cancers, which could be an attractive therapeutic target [8, 10-13]. PI3K $\alpha$  comprises a catalytic subunit, p110 $\alpha$ , and a regulatory subunit, p85 $\alpha$ . The p110 $\alpha$  subunit consists of five domains, namely adaptor-binding domain, RAS-binding domain, and the C2, helical, and kinase domains [14]. The gene encoding p110 $\alpha$  is frequently mutated in a variety of human tumors, including breast, colon and endometrial cancers, and glioblastomas [15-20]. Nearly 80% of the mutations were clustered in two hotspots [21-23]. One is located in the helical domain of p110 $\alpha$  (E542K, E545K and Q546K), which activates PI3K $\alpha$  by relieving the auto-inhibition imposed by the p85 $\alpha$  nSH2 domain on the p110 $\alpha$  subunit [24-26]. Another hotspot (H1047R) is located in the kinase domain, which induces conformational changes that increase PI3K $\alpha$  membrane association and lipid binding [27-29]. These two hotspot mutations act synergistically, but work independently to induce aberrant PI3K activity and malignant transformation in cancer cells [30]. Inhibition of PI3K $\alpha$  is a promising approach to kill or, at least, greatly inhibit the growth of cancer cells [31-36].

To date, several inhibitors targeting PI3K have been developed, some of them are under preclinical evaluation or early clinical studies [37-40]. **BKM120**, a pan-PI3K inhibitor, is one of the most advanced drug lead in clinical trials for solid tumors [41, 42], which is active against a number of tumor types [43], however, such broad anticancer activities usually result in potential risk of adverse events, including hyperglycemia and liver toxicity [41, 44]. **BYL-719**, a PI3K $\alpha$  inhibitor, exhibited strong antitumor activities *in vitro* and tumor xenograft models, and is particularly effective against cancer cell lines with mutant or amplified PIK3CA (PI3K, catalytic, alpha polypeptide) [45-47]. Therefore, targeting the PI3K $\alpha$  mutant enzyme may be a

promising approach to develop efficacious inhibitors [48]. Recently, many groups have demonstrated that PIK3CA mutations occur at high frequency in all kinds of solid tumors [40, 49]. Moreover, most of the mutations concentrate on the two hotspots [40, 50, 51]. Specific inhibitors that target the mutant forms of PI3K $\alpha$  could enhance treatment efficiency while decreasing various side-effects [52].

Although mutant selective inhibitors have significant advantages, the discovery of such inhibitors remains a great challenge [22]. *Via* a high-throughput screening campaign, an in-house library with diverse chemical structures was screened against the PI3K $\alpha$  H1047R mutant protein, from which **Hit-01** (**Figure 1**) was identified to weakly inhibit the enzyme function [53]. Herein, we report the synthesis, biological evaluation and structure–activity relationship analysis of a series of **Hit-01** analogues as novel PI3K $\alpha$  H1047R mutant inhibitors with greatly improved potency.

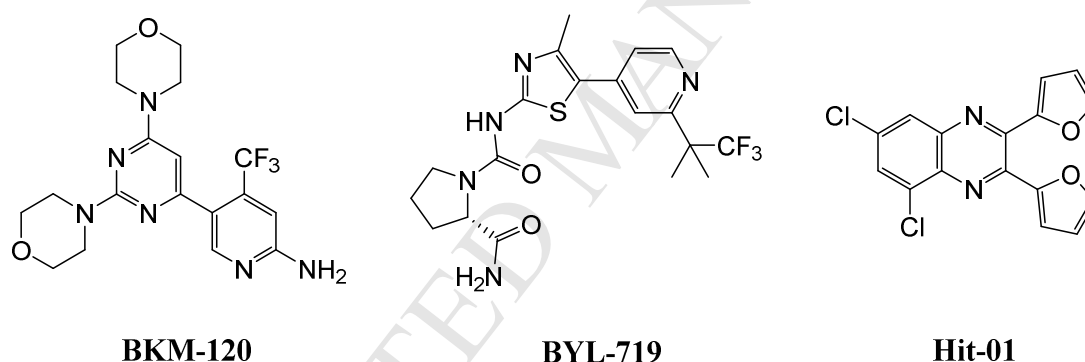
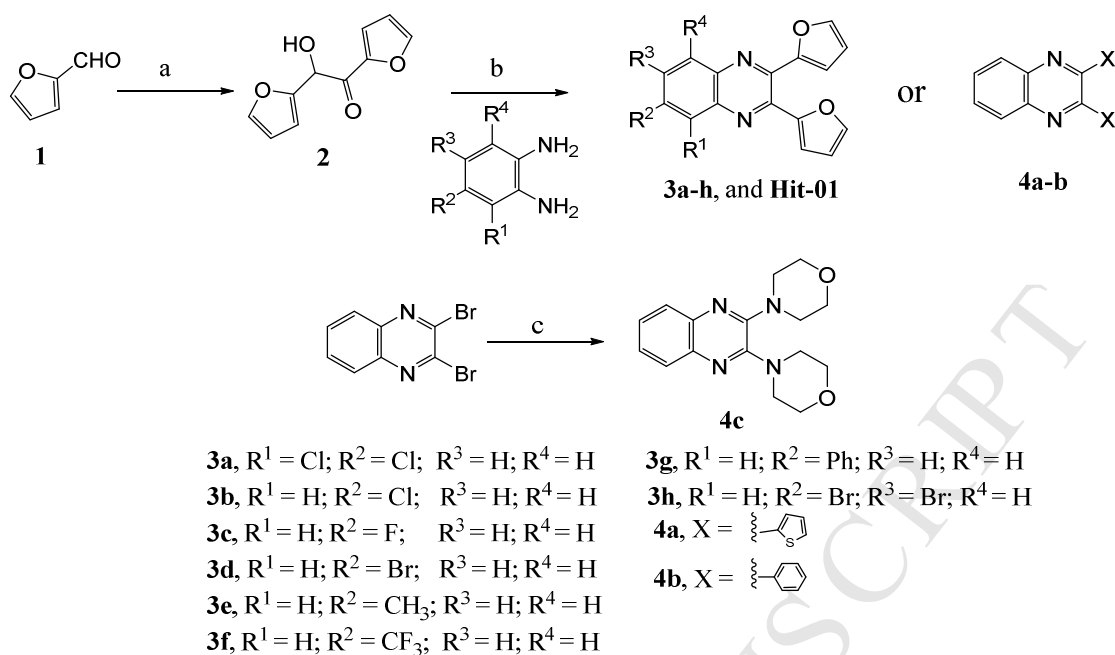


**Figure 1** Chemical structures of reported PI3Ks inhibitors and **Hit-01**

## 2. Results and discussion

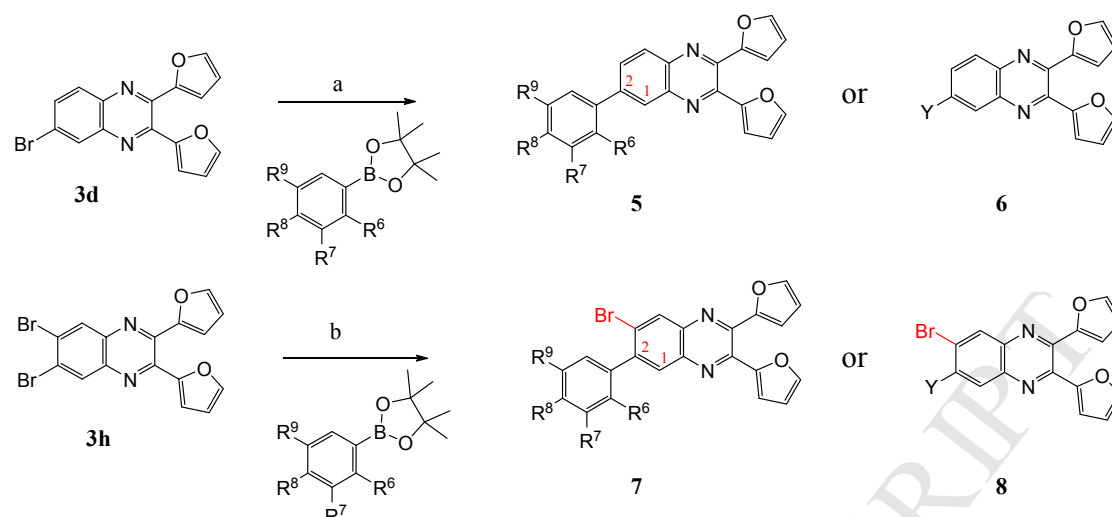
### 2.1 Chemistry

**Hit-01** contains a quinoxaline core with two appending furan rings. First, we synthesized **Hit-01** and its analogues with the reaction of furoin (**2**) using 3,5-dichlorobenzene-1,2-diamine catalyzed by amberlyst-15 (**Scheme 1**). To identify the optimal substitutions on the quinoxaline core, analogues with various halo-substitutions (**3a-h**) were synthesized with yields ranging from 46 to 78%. In addition, to explore whether the two furan groups are essential for biological activities, we prepared **4a-c**, with thienyl (**4a**), phenyl (**4b**), and morpholinyl (**4c**) moieties attaching to the quinoxaline core respectively.



**Scheme 1** Reagents and conditions: (a) Et<sub>3</sub>N, THF/H<sub>2</sub>O = 1/4, 1,3-dimethylbenzimidazolium iodide, reflux, overnight, 83%; (b) Amberlyst-15, H<sub>2</sub>O, reflux, 6 h, 46-78%; (c) Pd<sub>2</sub>(dba)<sub>3</sub>, BINAP, K<sub>2</sub>CO<sub>3</sub>, dioxane, overnight.

With the improved enzymatic potencies for **3d**, **3g** and **3h** (Table 1), we made further efforts to enhance their activities. As shown in Scheme 2, target compounds **5a-d** and **6a-c** were successfully prepared by the Suzuki reaction of **3d** with various benzyl borates using Pd<sub>2</sub>(dba)<sub>3</sub> as the catalyst and XPhos as a ligand, respectively. However, we failed to obtain compounds **7a-n** and **8a-e** using the same reagents and conditions. The reaction led only to bis-substitution of the two bromine atoms or elimination of bromine in **3h**. Significant efforts were made to optimize the reaction, and we eventually found that Pd(OAc)<sub>2</sub>, s-phos and K<sub>3</sub>PO<sub>4</sub> were the best combination to accomplish the transformation smoothly, and **7a-n** and **8a-e** were thus obtained with satisfactory yields (32-59%).



<b>5a</b>	R <sup>6</sup> = F	R <sup>7</sup> = H	R <sup>8</sup> = H	R <sup>9</sup> = H	<b>6a</b>	Y =	<b>8a</b>	Y =	<b>8d</b>	Y =
<b>5b</b>	R <sup>6</sup> = OMe	R <sup>7</sup> = H	R <sup>8</sup> = H	R <sup>9</sup> = H	<b>6b</b>	Y =	<b>8b</b>	Y =	<b>8e</b>	Y =
<b>5c</b>	R <sup>6</sup> = OH	R <sup>7</sup> = H	R <sup>8</sup> = H	R <sup>9</sup> = H	<b>6c</b>	Y =	<b>8c</b>	Y =		
<b>5d</b>	R <sup>6</sup> = CF <sub>3</sub>	R <sup>7</sup> = H	R <sup>8</sup> = H	R <sup>9</sup> = H						
<b>7a</b>	R <sup>6</sup> = H	R <sup>7</sup> = H	R <sup>8</sup> = H	R <sup>9</sup> = H	<b>7h</b>	R <sup>6</sup> = Cl	R <sup>7</sup> = H	R <sup>8</sup> = H	R <sup>9</sup> = H	
<b>7b</b>	R <sup>6</sup> = F	R <sup>7</sup> = H	R <sup>8</sup> = H	R <sup>9</sup> = H	<b>7i</b>	R <sup>6</sup> = Br	R <sup>7</sup> = H	R <sup>8</sup> = H	R <sup>9</sup> = H	
<b>7c</b>	R <sup>6</sup> = H	R <sup>7</sup> = F	R <sup>8</sup> = H	R <sup>9</sup> = H	<b>7j</b>	R <sup>6</sup> = OH	R <sup>7</sup> = H	R <sup>8</sup> = H	R <sup>9</sup> = H	
<b>7d</b>	R <sup>6</sup> = H	R <sup>7</sup> = H	R <sup>8</sup> = F	R <sup>9</sup> = H	<b>7k</b>	R <sup>6</sup> = OMe	R <sup>7</sup> = H	R <sup>8</sup> = H	R <sup>9</sup> = H	
<b>7e</b>	R <sup>6</sup> = F	R <sup>7</sup> = F	R <sup>8</sup> = H	R <sup>9</sup> = H	<b>7l</b>	R <sup>6</sup> = H	R <sup>7</sup> = H	R <sup>8</sup> = CF <sub>3</sub>	R <sup>9</sup> = H	
<b>7f</b>	R <sup>6</sup> = F	R <sup>7</sup> = H	R <sup>8</sup> = F	R <sup>9</sup> = H	<b>7m</b>	R <sup>6</sup> = H	R <sup>7</sup> = H	R <sup>8</sup> = OMe	R <sup>9</sup> = H	
<b>7g</b>	R <sup>6</sup> = CF <sub>3</sub>	R <sup>7</sup> = H	R <sup>8</sup> = H	R <sup>9</sup> = H	<b>7n</b>	R <sup>6</sup> = H	R <sup>7</sup> = OMe	R <sup>8</sup> = H	R <sup>9</sup> = OMe	

**Scheme 2** Reagents and conditions: (a) Pd<sub>2</sub>(dba)<sub>3</sub>, XPhos, K<sub>2</sub>CO<sub>3</sub>, dioxane, overnight, yields: 38-57%. (b) Pd(OAc)<sub>2</sub>, s-Phos, K<sub>3</sub>PO<sub>4</sub>, *t*-BuOH/H<sub>2</sub>O = 20/1, 80 °C, 2.5-4 h, yields: 32-59%.

## 2.2 Inhibition of PI3K $\alpha$ H1047R mutated kinase and cell proliferation

All synthesized compounds were evaluated for their antiproliferative activities on PI3K $\alpha$  H1047R mutated cell line HCT-116 and a PI3K $\alpha$  H1047R non-mutation cancer cell line MCF-7, as well as their inhibitory potency against PI3K $\alpha$  H1047R mutated kinase. The ZSTK474 and DOX were used as positive control compounds in the cell viability assay, and results of the biological evaluation are summarized in **Table 1**.

For the first series of compounds **3a-h**, the substitutions of R<sup>1</sup>-R<sup>4</sup> played important roles for exerting their enzymatic inhibitory activities. Compared with **Hit-01**, compound **3a** with a chlorine atom relocated from position 3 to 2 of the quinoxaline core totally lost its biochemical activity. However, removal of the chlorine atom at position 1 of the quinoxaline core afforded **3b** with much improved activity. This observation suggested that substitutions at position 2 might enhance compounds'

potencies. Thus, different groups were introduced to position 2 on the quinoxaline core. Compounds **3c**, **3e** and **3f** were inactive, while **3d**, **3g** and **3h** exhibited weak activities. In addition, to explore whether the two furan rings appending to the quinoxaline core are essential for biological activities, heterocyclic or aryl groups were incorporated into **Hit-01**. To our disappointment, all these analogues (**4a-c**) lost their inhibitory properties.

**Table 1** Inhibitory activities of quinoxalines against two cancer cell lines and PI3K $\alpha$  H1047R mutated kinase

Compound	EC <sub>50</sub> ( $\mu$ M)	IC <sub>50</sub> ( $\mu$ M) <sup>a</sup>	
	PI3K $\alpha$ (H1047R)	HCT-116	MCF-7
<b>Hit-01</b>	76.0 $\pm$ 5.7	> 50	> 50
<b>3a</b>	> 100	> 50	> 50
<b>3b</b>	18.1 $\pm$ 3.9	> 50	> 50
<b>3c</b>	> 100	> 50	> 50
<b>3d</b>	33.5 $\pm$ 3.6	> 50	> 50
<b>3e</b>	> 100	> 50	> 50
<b>3f</b>	> 100	> 50	> 50
<b>3g</b>	47.8 $\pm$ 4.5	> 50	> 50
<b>3h</b>	39.3 $\pm$ 5.2	> 50	> 50
<b>4a</b>	> 100	> 50	> 50
<b>4b</b>	> 100	> 50	> 50
<b>4c</b>	> 100	> 50	> 50
<b>5a</b>	12.7 $\pm$ 2.7	39.7 $\pm$ 3.2	> 50
<b>5b</b>	87.3 $\pm$ 4.8	> 50	> 50
<b>5c</b>	43.5 $\pm$ 4.2	> 50	> 50
<b>5d</b>	11.8 $\pm$ 1.1	45.3 $\pm$ 3.9	> 50
<b>6a</b>	> 100	> 50	> 50
<b>6b</b>	> 100	> 50	> 50
<b>6c</b>	> 100	> 50	> 50
<b>7a</b>	20.5 $\pm$ 2.3	> 50	> 50
<b>7b</b>	0.137 $\pm$ 0.03	11.23 $\pm$ 1.33	13.66 $\pm$ 2.18
<b>7c</b>	2.9 $\pm$ 0.5	43.07 $\pm$ 2.35	19.56 $\pm$ 3.96
<b>7d</b>	1.9 $\pm$ 0.4	38.05 $\pm$ 3.12	35.07 $\pm$ 2.76
<b>7e</b>	7.3 $\pm$ 0.7	> 50	> 50
<b>7f</b>	3.2 $\pm$ 0.7	16.55 $\pm$ 1.02	27.94 $\pm$ 3.28
<b>7g</b>	0.169 $\pm$ 0.06	13.46 $\pm$ 2.77	15.51 $\pm$ 2.54
<b>7h</b>	> 100	> 50	> 50
<b>7i</b>	> 100	> 50	> 50
<b>7j</b>	> 100	> 50	> 50
<b>7k</b>	> 100	> 50	> 50
<b>7l</b>	0.516 $\pm$ 0.07	14.9 $\pm$ 1.69	25.18 $\pm$ 1.32

<b>7m</b>	> 100	> 50	> 50
<b>7n</b>	> 100	> 50	> 50
<b>8a</b>	10.8 ± 1.1	45.7 ± 2.21	> 50
<b>8b</b>	> 100	> 50	> 50
<b>8c</b>	1.2 ± 0.4	38.5 ± 4.67	40.9 ± 3.36
<b>8d</b>	13.5 ± 0.9	> 50	> 50
<b>8e</b>	18.6 ± 1.0	> 50	> 50
ZSTK474	0.05 ± 0.01	1.31 ± 0.24	5.27 ± 0.73
DOX	ND	1.96 ± 0.09	3.28 ± 0.52

<sup>a</sup> Values are average of three independent experimental measurements and expressed as Mean ± SD. ND: not determined.

Inspired by the above observations, we conducted further modifications on compounds **3d** and **3h**. As shown in **Table 1**, compounds **5a-d** displayed moderate enzyme inhibitory activities, and **5a** and **5d** showed improved activities as compared to **Hit-01**. Replacing the substituted-phenyl group at position 2 of the quinoxaline core by polar heterocyclic moieties generated compounds **6a-c**, which lost their ability to inhibit the enzymatic function as well as cancer cell growth. In this round of SAR campaign, the most potent compound (**5d**) showed an EC<sub>50</sub> value of 11.8 μM against PI3Kα H1047R protein, which is far from satisfaction. Thus, we continued our structural modifications on **Hit-01** with the aim to further improve its biochemical potency.

As shown in **Table 1**, compounds **7a-g** and **7l** displayed not only improved EC<sub>50</sub> value for inhibiting the mutated kinase function, but also showed enhanced anti-proliferative activities against cancer cells. Among this series, compound **7b** demonstrated the best inhibitory activity for PI3Kα H1047R mutant (EC<sub>50</sub> = 0.137 μM). Moreover, **7b** exhibited potent antiproliferative activities for HCT116 (IC<sub>50</sub> = 11.23 μM) and MCF-7 (IC<sub>50</sub> = 13.66 μM) cells, respectively. However, compounds **7c** and **7d**, with a fluorine atom at meta- and para- position of the phenyl ring respectively showed reduced activities, suggesting that fluorine substitutions on the phenyl ring had a detrimental effect on the potency. Besides, compound **7g** (EC<sub>50</sub> = 0.169 μM for PI3Kα H1047R mutant) also showed a similar inhibition effect as **7b**, which means trifluoromethyl group was another favorable substitution. To figure out whether para-substitution on phenyl ring affect the activity, compounds **7l** and **7m**

were synthesized and the results suggested that an electron-drawing R<sup>8</sup> (**7l**, EC<sub>50</sub> = 0.516 μM) was beneficial for the potency, while introduction of an electron-donating group (-OCH<sub>3</sub>) resulted in a complete loss of activity (**7m**). At last, polar heterocyclic groups were introduced into **3h**, the resulting compounds **8a-e** showed decreased activities. In all, we modified **Hit-01** and identified two potent compounds **7b** and **7g**, which strongly inhibited PI3Kα H1047R mutant and cancer cell proliferation. Since these compounds displayed similar anti-proliferative activities on both PI3Kα H1047R mutated cell line HCT-116 and PI3Kα non-mutation cancer cell line MCF-7, these compounds may inhibit both PI3Kα H1047R mutant and PI3Kα wild-type proteins.

**Table 2.** Inhibitory activity (EC<sub>50</sub>, μM) against PI3Kα wild type and H1047R mutant.

Compounds	PI3Kα wild-type	PI3Kα H1047R	SI <sup>b</sup>
	EC <sub>50</sub> (μM) <sup>a</sup>	EC <sub>50</sub> (μM) <sup>a</sup>	
<b>Hit-01</b>	54.6 ± 6.5	76.0 ± 5.7	1.39
<b>3d</b>	27.6 ± 3.5	33.5 ± 3.6	1.21
<b>3g</b>	12.4 ± 2.1	47.8 ± 4.5	3.83
<b>5d</b>	12.8 ± 1.8	11.8 ± 1.1	0.92
<b>7b</b>	0.093 ± 0.05	0.137 ± 0.03	1.47
<b>7g</b>	0.097 ± 0.02	0.169 ± 0.06	1.74

<sup>a</sup> Values are average of three independent experimental determinations and the EC<sub>50</sub> values were expressed as Mean ± SD. <sup>b</sup> SI stands for selectivity index, which was calculated by comparing the EC<sub>50</sub> values of compounds inhibiting PI3Kα H1047R mutant against the EC<sub>50</sub> value of the same compound inhibiting PI3Kα wild-type in a biochemical assay.

To verify our hypothesis, some of the synthesized compounds were selected and measured for their inhibitory activity against PI3Kα wild-type and the mutant. As expected, all selected compounds showed similar inhibitory activities against PI3Kα wild-type and H1047R mutant (**Table 2**). Of note, compounds **7b** and **7g** displayed the best potencies against these two proteins, with EC<sub>50</sub> values of 0.093 and 0.097 μM against PI3Kα wild type, and 0.137 and 0.167 μM against PI3Kα H1047R mutant,

respectively. Although compounds **7b** and **7g** did not exhibit selectivity index on the PI3K $\alpha$  wild type and mutant proteins, they could be used as novel and potent PI3K $\alpha$  inhibitors. Then we compared the biochemical activities of **7b** with other isoforms of PI3K and mTORC1. As summarized in Table 3, **7b** displayed relative weak inhibitory potencies against other PI3K isoforms, with over 40-fold selectivity for  $\alpha$  over  $\beta$ , and over 100-fold for  $\alpha$  over  $\gamma$  and  $\delta$ . Meanwhile, **7b** have little effect on mTORC1 function when the tested concentration up to 30  $\mu$ M.

Table 3. Enzymatic activities of compound **7b** against PI3Ks and mTORC1 (IC<sub>50</sub>,  $\mu$ M<sup>a</sup>)

Kinase	Compound <b>7b</b>	BEZ-235	ZSTK474
PI3K $\alpha$	0.093 $\pm$ 0.05	0.040 $\pm$ 0.01	0.050 $\pm$ 0.017
PI3K $\beta$	3.34 $\pm$ 0.13	0.015 $\pm$ 0.003	0.044 $\pm$ 0.014
PI3K $\gamma$	9.89 $\pm$ 0.41	0.067 $\pm$ 0.021	0.051 $\pm$ 0.018
PI3K $\delta$	15.67 $\pm$ 0.52	0.093 $\pm$ 0.032	0.010 $\pm$ 0.004
mTORC1	> 30	0.079 $\pm$ 0.024	ND

<sup>a</sup> Values are average of three independent experimental determinations. ND: not determined.

### 2.3 Cell cycle arrest

Since **7b** showed the highest potency, we next conducted additional studies to investigate its biological roles in HCT116 cancer cell. We examined the effect of compound **7b** on cell cycle distribution using the propidium iodide (PI) staining kit. HCT116 cells were treated with compound **7b** (5, 10, 20  $\mu$ M) or control for 24 h, stained with PI and then analyzed on a flow cytometer.

As shown in **Figure 2**, compound **7b** led to a significant accumulation of cells at G1 phase from 38.72% to 44.42% (5  $\mu$ M), 57.67% (10  $\mu$ M) and 70.72% (20  $\mu$ M), accordingly. At the same time, it reduced the cells at S phase from 29.81 to 18.28%, and G2 phase from 31.47% to 11.00%, respectively. Meanwhile, we found that cell cycle arrest at G1 phase induced by compound **7b** was concentration-dependent, which might be one of the possible mechanisms for its cytotoxicity.

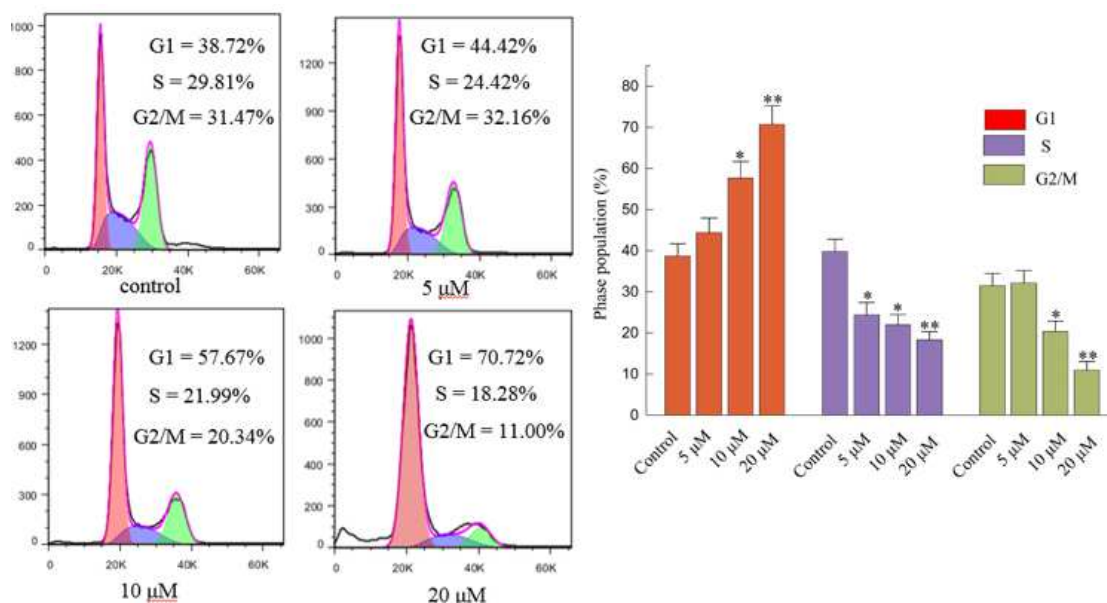


**Figure 2** Compound **7b** induced cell cycle arrest in the HCT-116 cell. Cells were treated with 5, 10 and 20  $\mu\text{M}$  of **7b** for 24 h, which were then harvested, washed with PBS, and fixed with 70% ice-cold ethanol at 4  $^{\circ}\text{C}$ . After overnight incubation, the cell pellets were collected by centrifugation, resuspended in 50  $\mu\text{g}/\text{mL}$  of RNase A in PBS, and incubated at 37  $^{\circ}\text{C}$  for 1 h. Next, PI dye (50  $\mu\text{g}/\text{mL}$ ) was added, and the mixture was incubated at 37  $^{\circ}\text{C}$  for 15 min. Cell cycle analysis was performed *via* PI fluorescence and flow cytometer. Data were expressed as Mean  $\pm$  SD (n= 3). \* $p < 0.05$  and \*\* $p < 0.01$  vs. the control.

## 2.4 Cell apoptosis

To explore the mechanism of cancer cells death, **7b** was used to induce HCT116 cell apoptosis, which were examined with Annexin V-FITC/PI FACS assay. As shown in **Figure 3**, the percentages of apoptotic population in HCT116 cells treated with **7b** at 6.25, 12.5 and 25  $\mu\text{M}$  for 24 h were 14.60, 18.50, and 37.74%, respectively, suggesting a dose-dependent apoptosis induction by **7b**.

To further explore the apoptosis mechanism by compound **7b** in HCT116 cells, we examined expression of caspase-3, caspase-8 and caspase-9 after **7b** treatment. Caspase-8 is the most upstream protease. Once activated, caspase-8 would cleave and activate downstream effector caspases like caspase-9 and caspase-3, which are recognized as bio-markers for cell apoptosis. As shown in **Figure 4**, expression of caspase-3, caspase-8 and caspase-9 were increased in a dose-dependent manner after **7b** treatment, suggesting that the caspase activation pathway was involved in the induction of apoptosis in HCT116 cancer cells by this compound.

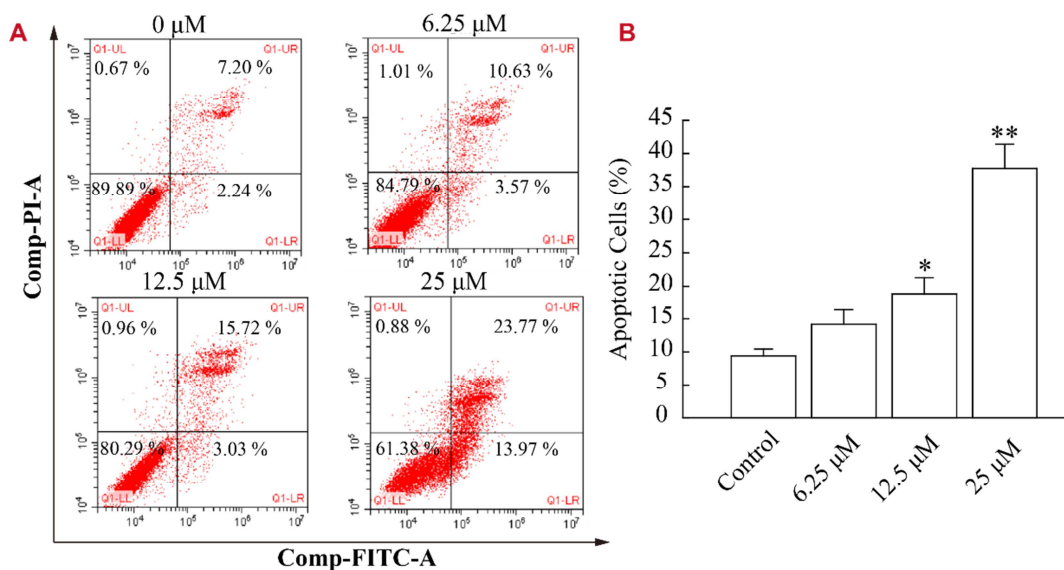


**Figure 3** Pro-apoptotic effect of compound **7b** on HCT116 cell. (A) Apoptotic assay by flow cytometry. HCT116 cell were treated with compound **7b** at 0, 6.25, 12.5, and 25  $\mu\text{M}$  for 24 h. Then cells were stained with Annexin V-FITC / PI, then detected by a flow cytometer. Cells in the upper right quadrant indicate PI positive / Annexin V positive, late apoptotic, or necrotic cells, and cells in the lower right quadrant indicate early apoptotic cells. (B) Bar graph represents statistics of total apoptotic cell percentages from three dependent experiments. \* $p < 0.05$  and \*\* $p < 0.01$  vs. the control.

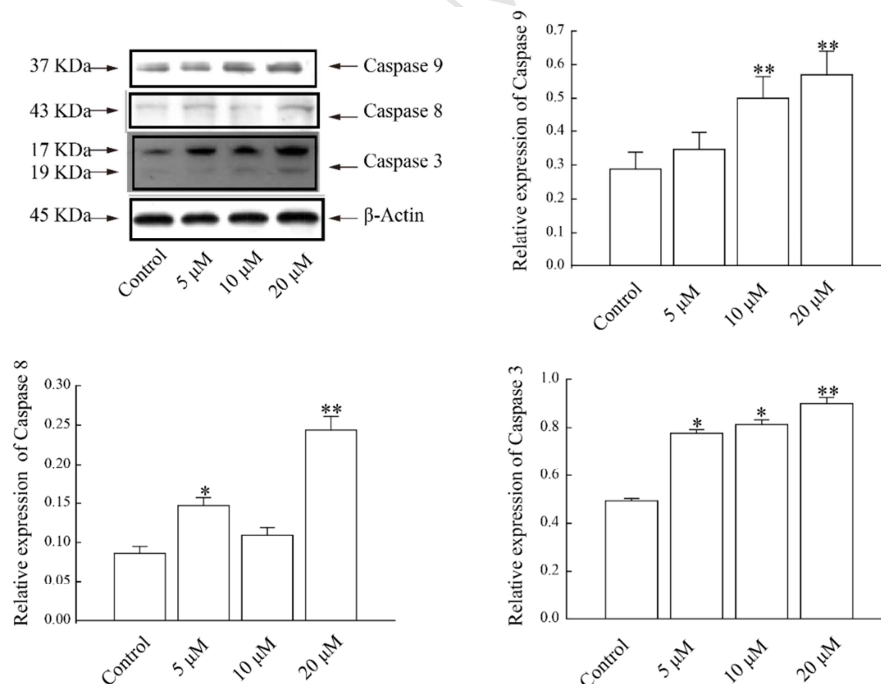


**Figure 4** Effects of compound **7b** on caspase-3, caspase-8 and caspase-9 expression. Cells were treated with compound **7b** for 72 h, then total protein was extracted and subjected to Western blot analysis,  $\beta$ -actin was used as an internal control. Bar graphs represent the expression level of Caspase proteins, which was quantified by an Image J software. Data were expressed as Means  $\pm$  SD (n = 3). \* $p < 0.05$  and \*\* $p < 0.01$ , vs. the control.

## 2.5 Inhibition of PI3K $\alpha$ H1047R mutant enzymatic activity by **7b**

Since **7b** inhibited PI3K $\alpha$  H1047R mutant, we docked **7b** into the PI3K $\alpha$  H1047R protein structure (PDB code: 3hhm), and found that **7b** formed hydrogen bond interactions with two important amino acids Lys802 and Asp933 (Figure 5). As both Lys802 and Asp933 play crucial roles in PI3K $\alpha$  phosphorylation, these interactions could potentially explain the inhibitory activities of **7b** on PI3K $\alpha$  function. To verify this hypothesis, we assessed *in vitro* PI3K $\alpha$  inhibitory activity of compound **7b** in cultured HCT116 cells. The cells were treated with **7b** at 5, 10 and 20  $\mu$ M, respectively, and subjected to Western blotting analysis. As expected, **7b** caused a decrease in *p*-AKT phosphorylation level (**Figure 6**), demonstrating that it is capable of inhibiting PI3K $\alpha$  H1047R activities.

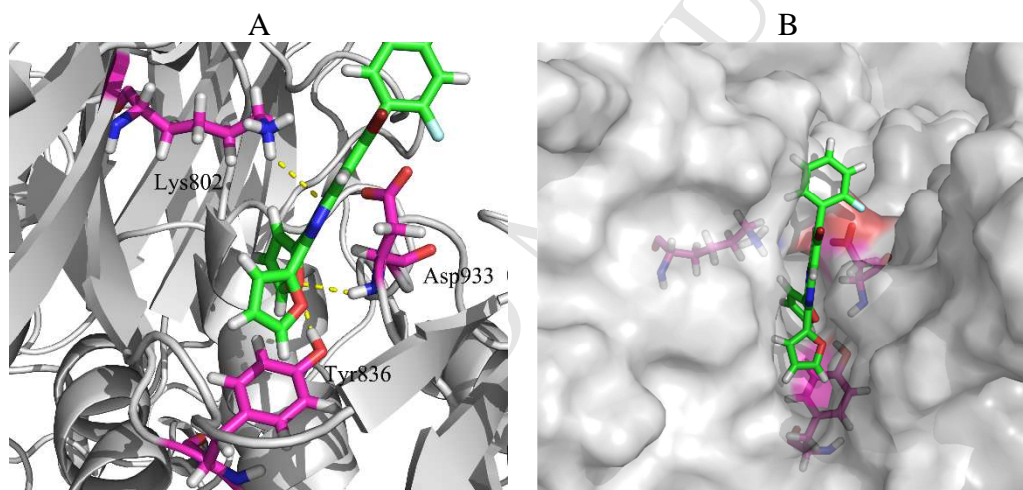


**Figure 5** Molecular docking of compound **7b** with the PI3K $\alpha$  H1047R mutant protein (PDB code: 3hhm). A, Docking model of **7b** in the binding pocket. B, Stereo view of **7b** in the binding pocket. Amino acid residues and compound **7b** are shown as stick models, H-bonds are shown as yellow dashed lines. The 3D graphical presentations were drawn by PyMol.

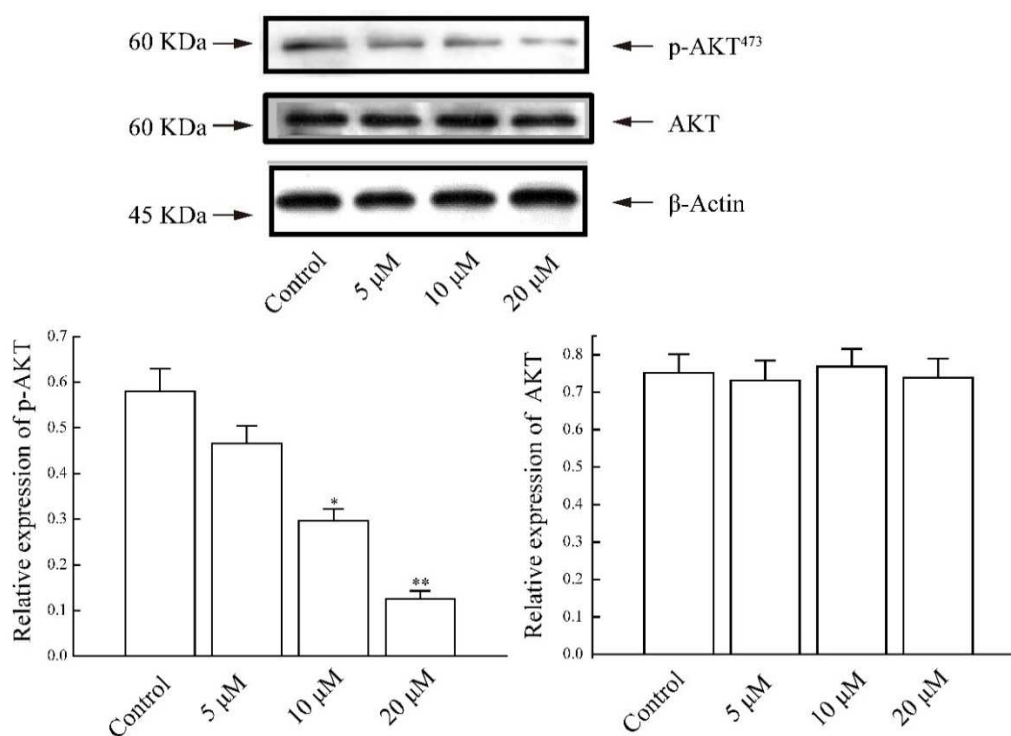


**Figure 6** Effects of compound **7b** on the AKT phosphorylation. Cells were treated with compound **7b** for 24 h, total protein was extracted and subjected to Western blot analysis, β-actin was used as an internal control. Bar graphs represent the expression level of AKT and p-AKT proteins, which were quantified by an Image J software. Data were expressed as Mean ± SD (n= 3). \* $p < 0.05$  and \*\* $p < 0.01$  vs. the control.

### 3. Conclusion

In conclusion, several series of novel compounds containing a quinoxaline core were synthesized and evaluated for their inhibitory effects on PI3K $\alpha$  H1047R mutant protein. Heterocyclic or aryl groups were incorporated into **Hit-01** to replace the two furan rings appending to the quinoxaline core. However, the resulting analogues (**4a-c**) lost their inhibitory properties, suggesting that the two furan groups are critical for its potency. This observation is in line with our docking studies. While keeping the furan rings and the quinoxaline core, we modified **3a**. The resulting analogues **5a** and **5d** bearing electron-withdrawing groups at the 2-position of benzene ring exhibited stronger inhibitory activities than the related analogues **5b-c** with electron-donating groups at the 2-position of benzene ring. Further SARs analysis enabled us to discover compound **7b**, which strongly inhibited both PI3K $\alpha$  H1047R mutant and wild-type

proteins with  $EC_{50}$  values of 0.137, and 0.093  $\mu$ M, respectively, while had little effect on other PI3K isoforms. Western blotting assay indicated that **7b** reduced the *p*-AKT phosphorylation level, demonstrating its inhibitory activity against the PI3K $\alpha$  H1047R mutant. Moreover, **7b** was docked well into the PI3K $\alpha$  H1047R mutant active site and formed strong hydrogen bonds with the protein. In addition, **7b** reduced HCT116 cancer cell proliferation with an  $IC_{50}$  of 11.23  $\mu$ M. Furthermore, studies on potential cytotoxic mechanisms indicated that compound **7b** could arrest cell cycle at G1 phase. Annexin V-FITC assay and Western blotting analysis revealed that compound **7b** induced HCT116 apoptosis by up-regulating caspase-3, caspase-8 and caspase-9 expressions. Wortmannin is a known and potent covalent pan-PI3K inhibitor. Its non-specificity led to side / off-target effects. Our results suggest that **7b** is a selective PI3K $\alpha$  inhibitor, which reversibly bind to the PI3K $\alpha$  pocket. With these superior properties, compound **7b** could be a promising lead for developing potent PI3K $\alpha$  inhibitors for cancer treatment.

## 4. Experimental section

### 4.1 Materials and methods

All chemicals were purchased from commercial sources and used as received. Reactions were monitored by thin-layer chromatography (TLC) and carried out on Merck Kieselgel 60 F<sub>254</sub> plates, which could be visualized under UV light at 254 nm. Column chromatography was performed on silica gel (60–120 mesh). All <sup>1</sup>H NMR spectra were obtained on an Agilent 400 MR spectrometer at ambient temperature and reported in ppm downfield from TMS (0 ppm). All <sup>13</sup>C NMR spectra were obtained with proton decoupling on an Agilent 400 MR DD2 (100 MHz) or 600 MR DD2 spectrometer and reported in ppm relative to CDCl<sub>3</sub> (77.16 ppm). Coupling constants were reported as Hz with multiplicity denoted as s (singlet), d (doublet), t (triplet), q (quartet), m (multiplet), and br (broad). The NMR data was processed by software Mest Re-Nova (Ver. 9.0.0.12821, Mestrelab Research S.L.). High resolution mass spectra (HRMS) were obtained on a Bruker Solarix 7.0T spectrometer. Melting point was recorded on a WRS-2A digital melting point apparatus. Compounds exhibited

purities of more than 95% as determined by peak area integration in reverse phase chromatography. The mobile phase is the mixtures of A and B, where A is 0.05% TFA water and B is acetonitrile, with a flow rate of 7 mL/min.

## 4.2 Chemical synthesis

4.2.1 General procedure for the preparation of 1,2-di(furan-2-yl)-2-hydroxyethan-1-one (**2**).

Furfural (10.0 mmol, 960 mg) and 1,3-dimethylbenzimidazolium iodide (5.0 mmol, 1370 mg) were dissolved in 25 mL THF/H<sub>2</sub>O (1/4). Then TEA (0.25 mL) was added, the mixture was heated to reflux for 5 h and cooled to room temperature. Ethyl acetate (50 mL) was added, the organic phase was washed with water (3 × 50 mL), dried over MgSO<sub>4</sub>, and concentrated. The crude products were purified by column chromatography, affording **2** (530 mg, 55% yield) as yellow solid. <sup>1</sup>H NMR (400 MHz, CDCl<sub>3</sub>) δ 7.61 (dd, *J* = 1.7, 0.8 Hz, 1 H), 7.37 (dd, *J* = 1.8, 0.8 Hz, 1 H), 7.25 (dd, *J* = 3.7, 0.8 Hz, 1 H), 6.40 (d, *J* = 3.3 Hz, 1 H), 6.54 (dd, *J* = 3.7, 1.7 Hz, 1 H), 6.35 (dd, *J* = 3.3, 1.9 Hz, 1 H), 5.80 (s, 1 H), 4.19 (s, 1 H). The data is in line with the literature reported previously [54].

4.2.2 General procedure for the preparation of compounds **3a-h** and **Hit-01**

Furoin **2** (1.0 mmol, 192 mg) and *o*-phenylenediamines (1.0 mmol) were dissolved in 3 mL H<sub>2</sub>O. Amberlyst-15 (100 mg) was added, the mixture was then heated to reflux for 10 h and cooled to room temperature. Ethyl acetate (10 mL) was added, the organic phase was washed with water (3 × 10 mL), dried over MgSO<sub>4</sub>, and concentrated. The crude products were purified by column chromatography, affording **3a-h** and **Hit-01**.

4.2.2.1 5,7-Dichloro-2,3-di(furan-2-yl)quinoxaline (**Hit-01**)

**Hit-01** was obtained as brown solid. Yield 69%. <sup>1</sup>H NMR (400 MHz, CDCl<sub>3</sub>) δ 8.04–7.84 (m, 1H), 7.61 (d, *J* = 15.8 Hz, 3H), 6.91–6.44 (m, 4H). <sup>13</sup>C NMR (100 MHz, CDCl<sub>3</sub>) δ 150.55, 150.15, 144.92, 144.55, 143.61, 142.48, 141.27, 136.01, 135.29, 133.87, 130.58, 126.94, 114.40, 114.12, 112.16, 112.11. HRMS (*m/z*): calcd for C<sub>16</sub>H<sub>9</sub>Cl<sub>2</sub>N<sub>2</sub>O<sub>2</sub> 330.9963 [M+H]<sup>+</sup>; found 330.9971.

4.2.2.2 5,6-Dichloro-2,3-di(furan-2-yl)quinoxaline (**3a**)

The product was obtained as brown solid. Yield 75%.  $^1\text{H}$  NMR (400 MHz,  $\text{CDCl}_3$ )  $\delta$  7.98–7.88 (m, 1H), 7.66–7.52 (m, 3H), 6.82 (dd,  $J = 3.5, 0.8$  Hz, 1H), 6.71 (dt,  $J = 3.6, 0.9$  Hz, 1H), 6.64–6.49 (m, 2H).  $^{13}\text{C}$  NMR (100 MHz,  $\text{CDCl}_3$ )  $\delta$  150.61, 150.24, 144.76, 144.68, 142.60, 142.60, 139.70, 138.74, 138.17, 134.50, 131.35, 127.97, 114.32, 114.00, 112.21, 112.07. HRMS ( $m/z$ ): calcd for  $\text{C}_{16}\text{H}_9\text{Cl}_2\text{N}_2\text{O}_2$  330.9963  $[\text{M}+\text{H}]^+$ ; found 330.9971.

4.2.2.3 6-Chloro-2,3-di(furan-2-yl)quinoxaline (**3b**)

The product was obtained as brown solid. Yield 71%.  $^1\text{H}$  NMR (400 M,  $\text{DMSO}-d_6$ ):  $\delta$  8.19 (1H,  $J = 2.1$  Hz, d), 8.16 (1H,  $J = 9.0$  Hz, d), 7.94–7.87 (3H, m), 6.78–6.72 (4H, m). The data is in line with the literature reported previously [55].

4.2.2.4 6-Fluoro-2,3-di(furan-2-yl)quinoxaline (**3c**)

The product was obtained as brown solid. Yield 78%.  $^1\text{H}$  NMR (400 MHz,  $\text{CDCl}_3$ )  $\delta$  8.11 (m, 1H), 7.74 (dd,  $J = 9.3, 3.1$  Hz, 1H), 7.64–7.57 (m, 2H), 7.50 (td,  $J = 8.5, 2.8$  Hz, 1H), 6.74–6.61 (m, 2H), 6.56 (m, 2H).  $^{13}\text{C}$  NMR (100 MHz,  $\text{CDCl}_3$ )  $\delta$  163.11 ( $J = 252$  Hz), 150.60, 150.50, 144.53, 144.14, 143.28, 141.93, 141.51, 141.38, 137.74, 131.19, 120.82, 113.60, 112.87, 112.68, 112.01. The data is in line with the literature reported previously [56].

4.2.2.5 6-Bromo-2,3-di(furan-2-yl)quinoxaline (**3d**)

The product was obtained as brown solid. Yield 55%.  $^1\text{H}$  NMR (400 MHz,  $\text{CDCl}_3$ )  $\delta$  8.31 (d,  $J = 2.1$  Hz, 1H), 7.98 (d,  $J = 8.9$  Hz, 1H), 7.80 (dd,  $J = 8.9, 2.1$  Hz, 1H), 7.62 (d,  $J = 1.6$  Hz, 2H), 6.70 (t,  $J = 3.3$  Hz, 2H), 6.57 (dd,  $J = 3.5, 1.8$  Hz, 2H).  $^{13}\text{C}$  NMR (100 MHz,  $\text{CDCl}_3$ )  $\delta$  150.55, 150.49, 144.52, 144.41, 143.20, 142.71, 141.10, 139.30, 133.84, 131.32, 130.29, 124.31, 113.63, 113.38, 112.03, 112.00. The data is in line with the literature reported previously [57].

4.2.2.6 2,3-Di(furan-2-yl)-6-methylquinoxaline (**3e**)

The product was obtained as brown solid. Yield 59%.  $^1\text{H}$  NMR (400 MHz,  $\text{CDCl}_3$ )  $\delta$  7.99 (d,  $J = 8.6$  Hz, 1H), 7.92–7.82 (m, 1H), 7.59 (d,  $J = 0.9$  Hz, 2H), 7.54 (dd,  $J = 8.6, 1.9$  Hz, 1H), 6.61 (d,  $J = 3.5$  Hz, 2H), 6.53 (m, 2H), 2.56 (s, 3H).  $^{13}\text{C}$  NMR (100

MHz, CDCl<sub>3</sub>)  $\delta$  150.92, 144.05, 143.93, 142.55, 141.81, 141.04, 140.69, 139.08, 132.71, 128.59, 127.93, 112.75, 112.50, 111.83, 111.80, 21.87. The data is in line with the literature reported previously [58].

#### 4.2.2.7 2,3-Di(furan-2-yl)-6-(trifluoromethyl)quinoxaline (**3f**)

The product was obtained as brown solid. Yield 46%. <sup>1</sup>H NMR (400 MHz, CDCl<sub>3</sub>)  $\delta$  8.42 (s, 1H), 8.21 (d,  $J$  = 8.8 Hz, 1H), 7.88 (dd,  $J$  = 8.9, 2.0 Hz, 1H), 7.63 (dd,  $J$  = 4.2, 1.7 Hz, 2H), 6.76 (dd,  $J$  = 7.5, 3.5 Hz, 2H), 6.58 (dt,  $J$  = 3.4, 1.6 Hz, 2H). <sup>13</sup>C NMR (100 MHz, CDCl<sub>3</sub>)  $\delta$  150.34, 144.84, 144.65, 144.10, 143.60, 139.47, 131.92, 131.59, 130.17, 127.05, 127.01, 125.86, 125.83, 114.23, 113.87, 112.14, 112.09. HRMS (m/z): calcd for C<sub>17</sub>H<sub>10</sub>F<sub>3</sub>N<sub>2</sub>O<sub>2</sub> 331.0616 [M+H]<sup>+</sup>; found 331.0610.

#### 4.2.2.8 2,3-Di(furan-2-yl)-6-phenylquinoxaline (**3g**)

The product was obtained as brown solid. Yield 55%. <sup>1</sup>H NMR (400 MHz, CDCl<sub>3</sub>):  $\delta$  8.39–8.35 (d, 1H,  $J$  = 2.0 Hz), 8.22–8.17 (d, 1H,  $J$  = 8.7 Hz), 8.06–8.01 (m, 1H), 7.80–7.75 (d, 2H,  $J$  = 7.2 Hz), 7.66–7.63 (s, 2H), 7.55–7.40 (m, 3H), 6.70–6.54 (m, 4H); The data is in line with the literature reported previously [57].

#### 4.2.2.9 6,7-Dibromo-2,3-di(furan-2-yl)quinoxaline (**3h**)

The product was obtained as brown solid. Yield 67%. <sup>1</sup>H NMR (400 MHz, CDCl<sub>3</sub>)  $\delta$  8.40 (s, 2H), 7.61 (d,  $J$  = 1.8 Hz, 2H), 6.72 (d,  $J$  = 3.5 Hz, 2H), 6.56 (dd,  $J$  = 3.6, 1.8 Hz, 2H). <sup>13</sup>C NMR (100 MHz, CDCl<sub>3</sub>)  $\delta$  150.33, 144.68, 143.31, 139.69, 132.95, 126.83, 113.96, 112.11. HRMS (m/z): calcd for C<sub>16</sub>H<sub>9</sub>Br<sub>2</sub>N<sub>2</sub>O<sub>2</sub> 418.8953 [M+H]<sup>+</sup>; found 418.8968.

#### 4.2.3.1 General procedure for the preparation of compound **4a**

Thenoin (1.0 mmol, 225 mg) and *o*-phenylenediamine (1.0 mmol) were dissolved in 3 mL H<sub>2</sub>O. Amberlyst (100 mg) was added, the mixture was then heated to reflux for 10 h and cooled to room temperature. Ethyl acetate (10 mL) was added, the organic phase was washed with water (3  $\times$  10 mL), dried over MgSO<sub>4</sub>, and concentrated. The crude products were purified by column chromatography, affording **4a**. Yield 49%. M.p. 129–130 °C; <sup>1</sup>H NMR (400 MHz, CDCl<sub>3</sub>)  $\delta$  8.10–8.07 (m, 2H), 7.75–7.72 (m, 2H), 7.50 (d,  $J$  = 5.2 Hz, 2H), 7.27–7.24 (m, 2H), 7.03–7.06 (m, 2H).

The data is in line with the literature reported previously [59].

#### 4.2.2.9 2,3-Diphenylquinoxaline (**4b**)

The product was obtained as brown solid. Yield 50%.  $^1\text{H}$  NMR (400 MHz, DMSO- $d_6$ ):  $\delta$  8.19–8.14 (2H, m), 7.95–7.81 (2H, m), 7.50–7.47 (4H, m), 7.45–7.33 (6H, m). The data is in line with the literature reported previously [60].

#### 4.2.3.2 General procedure for the preparation of compound **4c**

2,3-Dibromoquinoxaline (1.0 mmol, 285 mg) and morpholine (2.0 mmol, 180 mg) were dissolved into 5 mL dioxane, then  $\text{Pd}_2(\text{dba})_3$  (0.01 mmol), BINAP (0.02 mmol),  $\text{K}_2\text{CO}_3$  (2.0 mmol) were added to the mixture, respectively. The reaction was carried out at 80 °C in  $\text{N}_2$  atmosphere. After completion of the reaction, the mixture was cooled to room temperature and evaporated the solvent under reduced pressure. The affording crude product was purified by column chromatography to give **4c**. Yield 49%. M.p. 200–201 °C.  $^1\text{H}$  NMR (400 MHz, DMSO)  $\delta$  7.77–7.52 (m, 2H), 7.49–7.28 (m, 2H), 3.75 (t,  $J = 4.5$  Hz, 8H), 3.56–3.41 (m, 8H). The data matched the reported literature [61].

#### 4.2.4 General procedures for the preparation of compounds **5a–d** and **6a–c**.

Compound **3d** (1.0 mmol) and its borate (1.0 mmol) were added to 5 mL dioxane.  $\text{Pd}_2(\text{dba})_3$  (0.01 mmol), BINAP (0.02 mmol),  $\text{K}_2\text{CO}_3$  (2 mmol) were added to the mixture, respectively. The reaction was carried out at 80 °C in  $\text{N}_2$  atmosphere. After cooling to room temperature, the solvent of the mixture was evaporated under reduced pressure to afford crude product. Purification was made through column chromatography to give compounds **5a–d** and **6a–c**.

##### 4.2.4.1 6-(2-Fluorophenyl)-2,3-di(furan-2-yl)quinoxaline (**5a**)

The product was obtained as brown solid. Yield 57%.  $^1\text{H}$  NMR (400 MHz,  $\text{CDCl}_3$ )  $\delta$  8.32 (s, 1H), 8.18 (d,  $J = 8.7$  Hz, 1H), 7.97 (d,  $J = 8.9$  Hz, 1H), 7.61 (d,  $J = 13.6$  Hz, 3H), 7.39 (q,  $J = 6.9$  Hz, 1H), 7.32–7.16 (m, 3H), 6.68 (t,  $J = 3.6$  Hz, 2H), 6.58–6.48 (m, 2H).  $^{13}\text{C}$  NMR (100 MHz,  $\text{CDCl}_3$ )  $\delta$  161.14, 158.66, 150.80, 144.27, 144.23, 142.97, 142.70, 140.53, 139.96, 138.03, 131.69, 131.66, 130.83, 130.80, 130.02, 129.94, 128.91, 128.87, 128.84, 127.68, 127.55, 124.69, 124.66, 116.52, 116.29,

113.13, 113.09, 111.93. HRMS (m/z): calcd for  $C_{22}H_{14}FN_2O_2$  357.0973  $[M+H]^+$ ; found 357.0979.

#### 4.2.4.2 2,3-Di(furan-2-yl)-6-(2-methoxyphenyl)quinoxaline (**5b**)

The product was obtained as brown solid. Yield 57%.  $^1H$  NMR (400 MHz,  $CDCl_3$ )  $\delta$  8.30 (d,  $J = 2.0$  Hz, 1H), 8.15 (d,  $J = 8.7$  Hz, 1H), 7.99 (dd,  $J = 8.7, 2.0$  Hz, 1H), 7.78–7.68 (m, 2H), 7.67–7.57 (m, 2H), 7.13–6.97 (m, 2H), 6.66 (dd,  $J = 6.4, 3.4$  Hz, 2H), 6.56 (dt,  $J = 3.2, 1.5$  Hz, 2H), 3.87 (s, 3H).  $^{13}C$  NMR (100 MHz,  $CDCl_3$ )  $\delta$  159.96, 150.88, 150.82, 144.21, 144.10, 142.95, 142.66, 142.06, 140.96, 139.68, 131.86, 129.82, 129.27, 128.49, 125.41, 114.56, 113.00, 112.82, 111.90, 55.38. HRMS (m/z): calcd for  $C_{23}H_{17}N_2O_3$  369.1158  $[M+H]^+$ ; found 369.1163.

#### 4.2.4.3 2-(2,3-Di(furan-2-yl) quinoxaline-6-yl)phenol (**5c**)

The product was obtained as brown solid. Yield 42%.  $^1H$  NMR (400 MHz,  $DMSO-d_6$ )  $\delta$  9.89 (s, 1H), 8.22 (dt,  $J = 1.8, 0.9$  Hz, 1H), 8.09 (q,  $J = 1.1$  Hz, 2H), 7.89 (q,  $J = 1.2$  Hz, 2H), 7.48 (dd,  $J = 7.6, 1.6$  Hz, 1H), 7.35–7.22 (m, 1H), 7.11–6.90 (m, 2H), 6.81–6.58 (m, 4H).  $^{13}C$  NMR (100 MHz,  $DMSO-d_6$ )  $\delta$  155.15, 150.89, 150.87, 145.31, 145.29, 142.62, 142.16, 141.56, 140.33, 139.35, 133.16, 131.07, 130.08, 128.30, 128.25, 126.43, 120.24, 116.80, 113.21, 112.65, 112.62. HRMS (m/z): calcd for  $C_{22}H_{15}N_2O_3$  355.1004  $[M+H]^+$ ; found 355.1005.

#### 4.2.4.4 2,3-Di(furan-2-yl)-6-(2-(trifluoromethyl)phenyl)quinoxaline (**5d**)

The product was obtained as brown solid. Yield 55%.  $^1H$  NMR (400 MHz,  $CDCl_3$ )  $\delta$  8.15 (d,  $J = 8.7$  Hz, 1H), 8.09 (d,  $J = 1.9$  Hz, 1H), 7.81 (dd,  $J = 7.9, 1.3$  Hz, 1H), 7.71 (m, 1H), 7.66–7.59 (m, 3H), 7.58–7.49 (m, 1H), 7.43 (dd,  $J = 7.6, 1.4$  Hz, 1H), 6.69 (m, 2H), 6.57 (m, 2H).  $^{13}C$  NMR (100 MHz,  $CDCl_3$ )  $\delta$  150.78, 144.30, 144.25, 143.12, 142.88, 142.07, 139.96, 139.89, 139.81, 139.79, 131.86, 131.83, 131.81, 131.54, 128.97, 128.96, 128.69, 128.39, 128.30, 128.05, 126.32, 126.27, 125.37, 122.65, 113.16, 113.13, 111.94. HRMS (m/z): calcd for  $C_{23}H_{14}F_3N_2O_2$  407.1001  $[M+H]^+$ ; found 407.1004.

#### 4.2.4.5 2,3-Di(furan-2-yl)-6-(pyridin-4-yl)quinoxaline (**6a**)

The product was obtained as brown solid. Yield 38%.  $^1H$  NMR (400 MHz,  $CDCl_3$ )

$\delta$  8.85–8.69 (m, 2H), 8.42 (d,  $J = 2.0$  Hz, 1H), 8.23 (d,  $J = 8.7$  Hz, 1H), 8.02 (dd,  $J = 8.8, 2.1$  Hz, 1H), 7.71–7.66 (m, 2H), 7.64 (d,  $J = 1.7$  Hz, 2H), 6.73 (dd,  $J = 5.3, 3.5$  Hz, 2H), 6.58 (dd,  $J = 3.5, 1.8$  Hz, 2H).  $^{13}\text{C}$  NMR (100 MHz,  $\text{CDCl}_3$ )  $\delta$  150.64, 150.44, 149.27, 148.55, 146.87, 144.49, 143.31, 143.09, 140.66, 140.59, 139.73, 129.95, 128.98, 127.27, 121.73, 113.55, 113.46, 112.05, 112.03. HRMS (m/z): calcd for  $\text{C}_{21}\text{H}_{14}\text{N}_3\text{O}_2$  340.1012  $[\text{M}+\text{H}]^+$ ; found 340.1006.

#### 4.2.4.6 6-(Benzofuran-2-yl)-2,3-di(furan-2-yl)quinoxaline (**6b**)

The product was obtained as brown solid. Yield 45%.  $^1\text{H}$  NMR (400 MHz,  $\text{CDCl}_3$ )  $\delta$  8.56 (s, 1H), 8.13 (q,  $J = 8.8$  Hz, 2H), 7.68–7.45 (m, 4H), 7.38–7.04 (m, 4H), 6.69 (dd,  $J = 10.2, 3.4$  Hz, 2H), 6.57 (d,  $J = 4.0$  Hz, 2H);  $^{13}\text{C}$  NMR (100 MHz,  $\text{CDCl}_3$ )  $\delta$  155.28, 154.36, 150.79, 144.27, 143.16, 142.35, 140.79, 140.54, 132.02, 129.49, 128.93, 127.17, 125.13, 124.20, 123.20, 121.29, 113.20, 111.96, 111.93, 111.34, 103.80. HRMS (m/z): calcd for  $\text{C}_{24}\text{H}_{15}\text{N}_2\text{O}_3$  379.1004  $[\text{M}+\text{H}]^+$ ; found 379.1002.

#### 4.2.4.7 6-(Benzo[b]thiophen-2-yl)-2,3-di(furan-2-yl)quinoxaline (**6c**)

The product was obtained as brown solid. Yield 45%.  $^1\text{H}$  NMR (400 MHz,  $\text{CDCl}_3$ )  $\delta$  8.39 (s, 1H), 8.09 (q,  $J = 8.8$  Hz, 2H), 7.87–7.58 (m, 5H), 7.34 (q,  $J = 6.0, 4.9$  Hz, 2H), 6.68 (t,  $J = 3.9$  Hz, 2H), 6.57 (s, 2H).  $^{13}\text{C}$  NMR (100 MHz,  $\text{CDCl}_3$ )  $\delta$  150.77, 150.69, 144.34, 144.27, 143.20, 142.54, 142.36, 140.82, 140.48, 140.38, 139.97, 136.10, 129.48, 128.64, 125.60, 125.03, 124.73, 123.99, 122.34, 121.41, 113.26, 113.19, 111.97, 111.95. HRMS (m/z): calcd for  $\text{C}_{24}\text{H}_{15}\text{N}_2\text{O}_2\text{S}$  395.0783  $[\text{M}+\text{H}]^+$ ; found 395.0779.

### 4.2.5 General procedures for the preparation of compounds **7a–n** and **8a–e**

Compound **3h** (1.0 mmol) and its relative borates (1.0 mmol) were added to 5 mL dioxane.  $\text{Pd}(\text{OAc})_2$  (0.01 mmol), s-phos (0.02 mmol),  $\text{K}_3\text{PO}_4$  (2.0 mmol) were added to the mixture, which were then heated to 80 °C in  $\text{N}_2$  atmosphere. After completion of the reaction, the mixture was cooled to room temperature and evaporated the solvent under reduced pressure. The affording crude products were purified by column chromatography to give compounds **7a–n** and **8a–e**.

#### 4.2.5.1 6-Bromo-2,3-di(furan-2-yl)-7-phenylquinoxaline (**7a**)

The product was obtained as brown solid. Yield 43%.  $^1\text{H}$  NMR (400 MHz,  $\text{CDCl}_3$ )  $\delta$  8.49 (d,  $J = 1.0$  Hz, 1H), 8.09 (d,  $J = 1.0$  Hz, 1H), 7.63 (m, 2H), 7.55–7.39 (m, 6H), 6.72 (dd,  $J = 3.5, 0.9$  Hz, 2H), 6.58 (m, 2H).  $^{13}\text{C}$  NMR (100 MHz,  $\text{CDCl}_3$ )  $\delta$  150.64, 150.56, 144.73, 144.52, 144.42, 143.18, 140.05, 139.84, 139.46, 132.72, 130.34, 129.50, 128.24, 128.09, 125.49, 113.61, 113.42, 112.04, 112.01, 109.99. HRMS (m/z): calcd for  $\text{C}_{22}\text{H}_{14}\text{BrN}_2\text{O}_2$  417.0173  $[\text{M}+\text{H}]^+$ ; found 417.0168.

#### 4.2.5.2 6-Bromo-7-(2-fluorophenyl)-2,3-di(furan-2-yl)quinoxaline (**7b**)

The product was obtained as brown solid. Yield 45%.  $^1\text{H}$  NMR (400 MHz,  $\text{CDCl}_3$ )  $\delta$  8.49 (s, 1H), 8.08 (s, 1H), 7.63 (dd,  $J = 7.5, 1.7$  Hz, 2H), 7.53–7.39 (m, 1H), 7.42–7.34 (m, 1H), 7.32–7.14 (m, 2H), 6.73 (t,  $J = 3.2$  Hz, 2H), 6.58 (td,  $J = 3.9, 1.8$  Hz, 2H).  $^{13}\text{C}$  NMR (100 MHz,  $\text{CDCl}_3$ )  $\delta$  160.72, 158.25, 150.56, 144.59, 144.44, 143.41, 143.10, 140.42, 139.37, 139.24, 132.37, 131.26, 131.13, 130.55, 130.47, 126.16, 123.99, 115.89, 115.67, 113.76, 113.47, 112.04. HRMS (m/z): calcd for  $\text{C}_{23}\text{H}_{13}\text{BrFN}_2\text{O}_2$  435.0138  $[\text{M}+\text{H}]^+$ ; found 435.0141

#### 4.2.5.3 6-Bromo-7-(3-fluorophenyl)-2,3-di(furan-2-yl)quinoxaline (**7c**)

The product was obtained as brown solid. Yield 39%.  $^1\text{H}$  NMR (400 MHz,  $\text{CDCl}_3$ )  $\delta$  8.49 (s, 1H), 8.07 (s, 1H), 7.63 (d,  $J = 5.7$  Hz, 2H), 7.51–7.41 (m, 1H), 7.31–7.22 (m, 3H), 7.15 (td,  $J = 8.5, 2.5$  Hz, 1H), 6.73 (d,  $J = 3.4$  Hz, 2H), 6.59 (d,  $J = 4.3$  Hz, 2H).  $^{13}\text{C}$  NMR (100 MHz,  $\text{CDCl}_3$ )  $\delta$  163.50, 161.05, 150.56, 150.49, 144.61, 144.50, 143.37, 143.30, 143.22, 141.81, 141.73, 140.19, 139.35, 132.89, 130.41, 129.76, 129.68, 125.33, 125.30, 124.87, 116.81, 116.59, 115.34, 115.13, 113.80, 113.57, 112.08, 112.05. HRMS (m/z): calcd for  $\text{C}_{23}\text{H}_{13}\text{BrFN}_2\text{O}_2$  435.0138  $[\text{M}+\text{H}]^+$ ; found 435.0141

#### 4.2.5.4 6-Bromo-7-(4-fluorophenyl)-2,3-di(furan-2-yl)quinoxaline (**7d**)

The product was obtained as brown solid. Yield 41%.  $^1\text{H}$  NMR (400 MHz,  $\text{CDCl}_3$ )  $\delta$  8.47 (s, 1H), 8.05 (s, 1H), 7.63 (d,  $J = 4.8$  Hz, 2H), 7.49 (dd,  $J = 8.3, 5.3$  Hz, 2H), 7.17 (t,  $J = 8.5$  Hz, 2H), 6.72 (t,  $J = 4.1$  Hz, 2H), 6.65–6.50 (m, 2H).  $^{13}\text{C}$  NMR (100 MHz,  $\text{CDCl}_3$ )  $\delta$  163.96, 161.50, 150.58, 150.52, 144.56, 144.48, 143.61, 143.25, 143.18, 140.07, 139.41, 135.80, 135.77, 132.79, 131.33, 131.25, 130.36, 125.34,

115.27, 115.05, 113.70, 113.52, 112.06, 112.04. HRMS (m/z): calcd for  $C_{23}H_{13}BrFN_2O_2$  435.0138 [M+H]<sup>+</sup>; found 435.0141

#### 4.2.5.5 6-Bromo-7-(2,3-difluorophenyl)-2,3-di(furan-2-yl)quinoxaline (**7e**)

The product was obtained as brown solid. Yield 39%. <sup>1</sup>H NMR (400 MHz, CDCl<sub>3</sub>)  $\delta$  8.49 (s, 1H), 8.07 (s, 1H), 7.63 (dd,  $J = 7.0, 1.7$  Hz, 2H), 7.34–7.24 (m, 1H), 7.20 (m, 1H), 7.13 (m, 1H), 6.74 (d,  $J = 3.4$  Hz, 2H), 6.58 (td,  $J = 3.8, 1.8$  Hz, 2H). <sup>13</sup>C NMR (100 MHz, CDCl<sub>3</sub>)  $\delta$  150.55 ( $J = 287.8$  Hz), 150.54, 150.47, 147.87 ( $J = 247.4$  Hz), 144.67, 144.50, 143.60, 143.21, 140.57, 139.17, 137.99, 132.55, 131.20, 129.84, 126.15, 123.99, 117.73, 117.56, 113.91, 113.60, 112.09, 112.05. HRMS (m/z): calcd for  $C_{22}H_{12}BrF_2N_2O_2$  453.0044 [M+H]<sup>+</sup>; found 453.0047.

#### 4.2.5.6 6-Bromo-7-(2,4-difluorophenyl)-2,3-di(furan-2-yl)quinoxaline (**7f**)

The product was obtained as brown solid. Yield 40%. <sup>1</sup>H NMR (400 MHz, CDCl<sub>3</sub>)  $\delta$  8.48 (s, 1H), 8.05 (s, 1H), 7.63 (d,  $J = 6.6$  Hz, 2H), 7.35 (q,  $J = 7.7$  Hz, 1H), 6.99 (dt,  $J = 18.0, 8.1$  Hz, 2H), 6.73 (d,  $J = 3.5$  Hz, 2H), 6.58 (d,  $J = 4.2$  Hz, 2H). <sup>13</sup>C NMR (100 MHz, CDCl<sub>3</sub>)  $\delta$  150.55, 150.47, 144.64, 144.50, 143.51, 143.17, 140.47, 139.20, 138.35, 132.47, 132.27, 132.22, 132.17, 132.13, 131.31, 126.07, 113.86, 113.57, 112.09, 112.05, 111.47, 111.44, 111.26, 111.22, 104.53, 104.28, 104.02. HRMS (m/z): calcd for  $C_{23}H_{13}BrFN_2O_2$  435.0138 [M+H]<sup>+</sup>; found 435.0141

#### 4.2.5.7 6-Bromo-2,3-di(furan-2-yl)-7-(2-(trifluoromethyl)phenyl)quinoxaline (**7g**)

The product was obtained as brown solid. Yield 49%. <sup>1</sup>H NMR (400 MHz, CDCl<sub>3</sub>)  $\delta$  8.47 (s, 1H), 8.02 (s, 1H), 7.82 (d,  $J = 7.7$  Hz, 1H), 7.69–7.51 (m, 4H), 7.35 (d,  $J = 7.6$  Hz, 1H), 7.26 (d,  $J = 1.9$  Hz, 1H), 6.73 (dd,  $J = 6.2, 3.5$  Hz, 2H), 6.58 (m, 2H). <sup>13</sup>C NMR (150 MHz, CDCl<sub>3</sub>)  $\delta$  150.58, 150.49, 144.61, 144.44, 143.51, 143.21, 142.06, 140.40, 138.83, 138.42, 131.94, 131.63, 131.39, 130.38, 128.83, 128.63, 128.58, 126.18, 126.15, 126.11, 126.08, 113.78, 113.50, 112.06, 112.03. HRMS (m/z): calcd for  $C_{23}H_{13}BrF_3N_2O_2$  485.0107 [M+H]<sup>+</sup>; found 485.0102.

#### 4.2.5.8 6-Bromo-7-(2-chlorophenyl)-2,3-di(furan-2-yl)quinoxaline (**7h**)

The product was obtained as brown solid. Yield 49%. <sup>1</sup>H NMR (400 MHz, CDCl<sub>3</sub>)  $\delta$  8.49 (s, 1H), 8.02 (s, 1H), 7.63 (dd,  $J = 9.1, 1.7$  Hz, 2H), 7.53 (dd,  $J = 7.6, 1.8$  Hz,

1H), 7.45–7.29 (m, 4H), 7.26 (s, 2H), 6.77–6.67 (m, 2H), 6.58 (m, 2H). <sup>13</sup>C NMR (100 MHz, CDCl<sub>3</sub>) δ 150.64, 150.54, 144.59, 144.43, 143.41, 143.09, 142.56, 140.44, 139.27, 138.95, 133.43, 132.21, 130.94, 130.59, 129.80, 129.54, 126.65, 126.21, 113.73, 113.46, 112.06, 112.04. HRMS (m/z): calcd for C<sub>22</sub>H<sub>13</sub>BrClN<sub>2</sub>O<sub>2</sub> 450.9843 [M+H]<sup>+</sup>; found 450.9851.

#### 4.2.5.9 6-Bromo-7-(2-bromophenyl)-2,3-di(furan-2-yl)quinoxaline (**7i**)

The product was obtained as brown solid. Yield 43%. <sup>1</sup>H NMR (400 MHz, CDCl<sub>3</sub>) δ 8.49 (s, 1H), 8.00 (s, 1H), 7.75–7.68 (m, 1H), 7.63 (m, 2H), 7.43 (m, 1H), 7.33 (m, 2H), 6.73 (dd, *J* = 4.7, 3.6 Hz, 2H), 6.58 (m, 2H). <sup>13</sup>C NMR (100 MHz, CDCl<sub>3</sub>) δ 150.65, 150.55, 144.59, 144.43, 144.10, 143.40, 143.10, 140.98, 140.44, 139.28, 132.67, 132.22, 130.83, 130.46, 129.90, 127.25, 126.15, 123.45, 113.73, 113.47, 112.06, 112.04. HRMS (m/z): calcd for C<sub>22</sub>H<sub>13</sub>Br<sub>2</sub>N<sub>2</sub>O<sub>2</sub> 494.9338 [M+H]<sup>+</sup>; found 494.9342.

#### 4.2.5.10 2-(7-Bromo-2,3-di(furan-2-yl)quinoxaline-6-yl)phenol (**7j**)

The product was obtained as brown solid. Yield 40%. <sup>1</sup>H NMR (400 MHz, CDCl<sub>3</sub>) δ 8.41 (s, 1H), 8.00 (s, 1H), 7.60 (m, 2H), 7.36 (td, *J* = 7.6, 1.8 Hz, 1H), 7.21 (dd, *J* = 7.8, 1.8 Hz, 1H), 7.08–6.98 (m, 3H), 6.71 (m, 2H), 6.56 (m, 2H), 5.89 (s, 1H). <sup>13</sup>C NMR (100 MHz, CDCl<sub>3</sub>) δ 152.89, 150.31, 144.63, 144.59, 143.20, 142.89, 140.85, 140.10, 139.04, 132.56, 131.27, 130.73, 130.22, 127.04, 126.93, 120.50, 116.45, 113.90, 113.78, 112.09. HRMS (m/z): calcd for C<sub>22</sub>H<sub>14</sub>BrN<sub>2</sub>O<sub>3</sub> 433.0182 [M+H]<sup>+</sup>; found 433.0177.

#### 4.2.5.11 6-Bromo-2,3-di(furan-2-yl)-7-(2-methoxyphenyl)quinoxaline (**7k**)

The product was obtained as brown solid. Yield 40%. <sup>1</sup>H NMR (400 MHz, CDCl<sub>3</sub>) δ 8.46 (s, 1H), 8.04 (s, 1H), 7.62 (d, *J* = 8.0 Hz, 2H), 7.45 (t, *J* = 7.9 Hz, 1H), 7.25 (d, *J* = 4.0 Hz, 2H), 7.14–6.93 (m, 2H), 6.70 (dd, *J* = 5.5, 3.4 Hz, 2H), 6.57 (d, *J* = 4.4 Hz, 2H), 3.80 (s, 4H). <sup>13</sup>C NMR (100 MHz, CDCl<sub>3</sub>) δ 156.68, 150.77, 150.66, 144.41, 144.26, 143.04, 142.84, 142.54, 140.20, 139.48, 131.94, 130.76, 130.73, 129.98, 129.20, 127.38, 120.44, 113.40, 113.16, 111.97, 111.95, 110.95, 55.53. HRMS (m/z): calcd for C<sub>23</sub>H<sub>16</sub>BrN<sub>2</sub>O<sub>3</sub> 447.0339 [M+H]<sup>+</sup>; found 447.0335.

4.2.5.12 6-Bromo-2,3-di(furan-2-yl)-7-(4-(trifluoromethyl)phenyl)quinoxaline (**7l**)

The product was obtained as brown solid. Yield 59%. <sup>1</sup>H NMR (400 MHz, CDCl<sub>3</sub>) δ 8.51 (s, 1H), 8.08 (s, 1H), 7.75 (d, *J* = 8.0 Hz, 2H), 7.71–7.60 (m, 4H), 6.75 (t, *J* = 3.6 Hz, 2H), 6.59 (m, 2H). <sup>13</sup>C NMR (150 MHz, CDCl<sub>3</sub>) δ 150.48, 150.43, 144.66, 144.55, 143.48, 143.28, 143.25, 143.09, 140.28, 139.32, 132.99, 130.46, 130.26, 129.92, 125.17, 125.15, 125.12, 125.09, 124.54, 113.91, 113.67, 112.10, 112.07. HRMS (m/z): calcd for C<sub>23</sub>H<sub>13</sub>BrF<sub>3</sub>N<sub>2</sub>O<sub>2</sub> 485.0107 [M+H]<sup>+</sup>; found 485.0102.

4.2.5.13 6-Bromo-2,3-di(furan-2-yl)-7-(4-methoxyphenyl)quinoxaline (**7m**)

The product was obtained as brown solid. Yield 44%. <sup>1</sup>H NMR (400 MHz, CDCl<sub>3</sub>) δ 8.47 (s, 1H), 8.06 (s, 1H), 7.62 (m, 2H), 7.53–7.43 (m, 2H), 7.08–6.94 (m, 2H), 6.71 (t, *J* = 3.2 Hz, 2H), 6.57 (m, 2H), 3.88 (s, 3H). <sup>13</sup>C NMR (100 MHz, CDCl<sub>3</sub>) δ 159.63, 150.65, 150.59, 144.46, 144.40, 144.39, 143.07, 143.01, 139.90, 139.53, 132.70, 132.22, 130.80, 130.17, 125.89, 113.52, 113.37, 112.02, 112.00, 55.30. HRMS (m/z): calcd for C<sub>23</sub>H<sub>16</sub>BrN<sub>2</sub>O<sub>3</sub> 447.0339 [M+H]<sup>+</sup>; found 447.0335.

4.2.5.14 6-Bromo-7-(3,5-dimethoxyphenyl)-2,3-di(furan-2-yl)quinoxaline (**7n**)

The product was obtained as brown solid. Yield 34%. <sup>1</sup>H NMR (400 MHz, CDCl<sub>3</sub>) δ 8.48 (s, 1H), 8.10 (s, 1H), 7.69–7.55 (m, 2H), 7.26 (s, 1H), 6.72 (t, *J* = 3.2 Hz, 2H), 6.65 (d, *J* = 2.2 Hz, 2H), 6.63–6.50 (m, 3H), 3.84 (s, 7H). <sup>13</sup>C NMR (100 MHz, CDCl<sub>3</sub>) δ 160.36, 150.62, 150.56, 144.62, 144.52, 144.44, 143.21, 143.14, 141.61, 140.06, 139.36, 132.76, 130.20, 125.23, 113.64, 113.45, 112.04, 112.03, 107.75, 100.56, 55.46. HRMS (m/z): calcd for C<sub>24</sub>H<sub>18</sub>BrN<sub>2</sub>O<sub>4</sub> 477.0518 [M+H]<sup>+</sup>; found 477.0512.

4.2.5.15 6-Bromo-2,3-di(furan-2-yl)-7-(pyridin-4-yl)quinoxaline (**8a**)

The product was obtained as brown solid. Yield 30%. <sup>1</sup>H NMR (400 MHz, CDCl<sub>3</sub>) δ 8.80–8.69 (m, 2H), 8.50 (d, *J* = 2.1 Hz, 1H), 8.06 (d, *J* = 2.1 Hz, 1H), 7.64 (dd, *J* = 5.4, 1.8 Hz, 2H), 7.51–7.40 (m, 2H), 6.76 (dd, *J* = 5.4, 3.5 Hz, 2H), 6.59 (m, 2H). <sup>13</sup>C NMR (100 MHz, CDCl<sub>3</sub>) δ 150.44, 150.40, 149.35, 147.83, 144.77, 144.64, 143.72, 143.40, 141.56, 140.50, 139.30, 133.25, 130.45, 124.38, 123.65, 114.09, 113.81, 112.15, 112.11. HRMS (m/z): calcd for C<sub>21</sub>H<sub>13</sub>BrN<sub>3</sub>O<sub>2</sub> 418.0185 [M+H]<sup>+</sup>; found

418.0181.

#### 4.2.5.15 6-(Benzofuran-2-yl)-7-bromo-2,3-di(furan-2-yl)quinoxaline (**8b**)

The product was obtained as brown solid. Yield 34%.  $^1\text{H}$  NMR (400 MHz,  $\text{CDCl}_3$ )  $\delta$  8.75 (s, 1H), 8.50 (s, 1H), 7.76 (s, 1H), 7.72–7.61 (m, 3H), 7.55 (d,  $J = 8.2$  Hz, 1H), 7.42–7.34 (m, 1H), 7.31–7.20 (m, 1H), 6.75 (dd,  $J = 9.1, 3.5$  Hz, 2H), 6.58 (dt,  $J = 3.7, 1.8$  Hz, 2H).  $^{13}\text{C}$  NMR (100 MHz,  $\text{CDCl}_3$ )  $\delta$  154.63, 152.01, 150.61, 150.54, 144.66, 144.50, 143.49, 143.37, 140.04, 139.28, 134.03, 132.37, 129.26, 128.70, 125.59, 123.19, 122.00, 121.75, 113.93, 113.62, 112.10, 112.04, 111.23, 108.64. HRMS ( $m/z$ ): calcd for  $\text{C}_{24}\text{H}_{14}\text{BrN}_2\text{O}_3$  457.0117  $[\text{M}+\text{H}]^+$ ; found 457.0113.

#### 4.2.5.16 6-(Benzo[b]thiophen-2-yl)-7-bromo-2,3-di(furan-2-yl)quinoxaline (**8c**)

The product was obtained as brown solid. Yield 32%.  $^1\text{H}$  NMR (400 MHz,  $\text{CDCl}_3$ )  $\delta$  8.52 (d,  $J = 1.8$  Hz, 1H), 8.32 (d,  $J = 1.7$  Hz, 1H), 7.88 (m, 2H), 7.74–7.57 (m, 3H), 7.53–7.32 (m, 2H), 6.75 (d,  $J = 3.5$  Hz, 2H), 6.59 (dt,  $J = 4.8, 2.2$  Hz, 2H).  $^{13}\text{C}$  NMR (100 MHz,  $\text{CDCl}_3$ )  $\delta$  150.51, 150.48, 144.69, 144.56, 143.49, 143.38, 140.50, 140.45, 140.26, 139.71, 139.19, 137.27, 133.40, 131.59, 125.64, 124.94, 124.93, 124.63, 124.17, 122.13, 113.96, 113.67, 112.12, 112.07. HRMS ( $m/z$ ): calcd for  $\text{C}_{24}\text{H}_{14}\text{BrN}_2\text{O}_2\text{S}$  472.9953  $[\text{M}+\text{H}]^+$ ; found 472.9939.

#### 4.2.5.17 6-Bromo-2,3-di(furan-2-yl)-7-(pyrimidin-5-yl)quinoxaline (**8d**)

The product was obtained as brown solid. Yield 32%.  $^1\text{H}$  NMR (400 MHz,  $\text{CDCl}_3$ )  $\delta$  9.31 (s, 1H), 8.95 (s, 2H), 8.52 (s, 1H), 8.09 (s, 1H), 7.64 (dd,  $J = 5.3, 1.7$  Hz, 2H), 6.78 (t,  $J = 3.7$  Hz, 2H), 6.59 (td,  $J = 3.9, 1.8$  Hz, 2H).  $^{13}\text{C}$  NMR (100 MHz,  $\text{CDCl}_3$ )  $\delta$  158.18, 156.82, 150.36, 150.33, 144.86, 144.73, 143.87, 143.50, 140.72, 139.37, 137.28, 133.75, 133.37, 130.87, 124.15, 114.27, 113.97, 112.19, 112.14. HRMS ( $m/z$ ): calcd for  $\text{C}_{20}\text{H}_{12}\text{BrN}_4\text{O}_2$  419.0096  $[\text{M}+\text{H}]^+$ ; found 419.0102.

#### 4.2.5.18

Tert-butyl-2-(7-bromo-2,3-di(furan-2-yl)quinoxaline-6-yl)-1H-pyrrole-1-carboxylate (**8e**)

The product was obtained as brown solid. Yield 32%.  $^1\text{H}$  NMR (400 MHz,  $\text{CDCl}_3$ )  $\delta$  8.38 (s, 1H), 8.08 (s, 1H), 7.63 (dd,  $J = 4.4, 1.8$  Hz, 2H), 7.48 (dd,  $J = 3.4, 1.8$  Hz,

1H), 6.73 (dd,  $J = 12.2, 3.4$  Hz, 2H), 6.58 (dd,  $J = 3.5, 1.8$  Hz, 2H), 6.39–6.16 (m, 2H), 1.28 (s, 10H).  $^{13}\text{C}$  NMR (100MHz,  $\text{CDCl}_3$ )  $\delta$  150.63, 150.54, 148.75, 144.55, 144.39, 143.10, 142.93, 140.35, 139.26, 138.81, 131.46, 131.36, 130.25, 128.37, 122.35, 115.58, 113.67, 113.38, 112.06, 112.03, 110.75, 84.12, 27.49. HRMS ( $m/z$ ): calcd for  $\text{C}_{25}\text{H}_{21}\text{BrN}_3\text{O}_4$  506.0697  $[\text{M}+\text{H}]^+$ ; found 506.0700.

### 4.3 Cell culture

HCT116 and MCF7 cancer cell lines were purchased from Shanghai Cell Bank of Chinese Academy of Sciences (Shanghai, China). The cells were cultured in DMEM supplemented with 10% FBS, 1% penicillin and streptomycin at 37 °C in a 5%  $\text{CO}_2$  humidified atmosphere. Cells grown at exponential stage were used for all the biological experiments.

### 4.4 Cell viability

Cell viability was assessed by Cell Counting Kit-8 (Beyotime, Jiangsu, China) following manufacturer's instructions. Compounds were dissolved in DMSO and diluted with culture medium. Cells at a density of  $5 \times 10^3$  per well were seeded in 96-well plates and cultured overnight, which were then treated with either vehicle (1% DMSO PBS buffer) or desired concentrations of compounds (50, 25, 12.5, 6.25, 3.12, 1.56, 0.78 and 0.39  $\mu\text{M}$ ) for 72 h at 37 °C. Cell viability was measured by the CCK-8 kit and the absorbance was measured using a microplate reader (Bio-Rad Laboratories) at 450 nm. At last, resultant  $\text{OD}_{450 \text{ nm}}$  values were expressed as  $\text{IC}_{50}$  values, which were the mean values derived from three independent experiments.

### 4.5 Cell cycle

Cells were seeded in 6-well plates at density of  $1 \times 10^5$  cells/well and treated with different concentrations of compound **7b** (5, 10 and 20  $\mu\text{M}$ ) for 24 h at 37 °C. Then, cells were harvested and fixed in 70% precooled ethanol. The cells were then treated with RNase A, and stained by PI (Product #: C1052, Beyotime, Jiangsu, China). Finally, the suspended cells were analyzed with a flow cytometer (Accuri C6, BD Biosciences), a minimum total of 10,000 events were recorded. The data were

analyzed with the FlowJo.

#### 4.6 Cell apoptosis

HCT116 cells were seeded at a density of  $1 \times 10^5$  cells/well on each well of 6-well plates and allowed to grow overnight. Then the cells were treated with **7b** (5, 10 and 20  $\mu$ M) for 24 h, cells without treatment were used as control group. Then the cells were trypsinized, washed with cold PBS for three times, centrifuged at 1200 rpm for 5 min, and the supernatants were discarded. Then cells were stained by an Annexin-V-fluorescein isothiocyanate (FITC) kit in the binding buffer for 15 min at room temperature. Subsequently, the cells were labeled by PI and the apoptotic cells were measured by a flow cytometer (Accuri C6), data were analyzed with BD Accuri C6 Plus.

#### 4.7 Western blotting

After treating HCT116 cells with **7b** (5, 10 and 20  $\mu$ M) for 24 h, the total proteins were extracted and their concentrations were balanced to the same level using BCA Protein Assay Reagent (Beyotime, Jiangsu, China), followed by 8 min protein denaturation with SDS loading buffer at 100 °C. Proteins (30  $\mu$ g) were separated by sodium dodecyl sulfate-polyacrylamide (SDS-PAGE) electrophoresis and transferred onto polyvinylidene fluoride (PVDF) membranes, which were blocked with 5% fat-free dry milk in  $1 \times$  Tris-buffered saline (TBS) containing 0.05% Tween 20 for 2 h at room temperature. Then the membranes were incubated with AKT (Beyotime, no: AA326), caspase-3 (Beyotime, no: AC030), caspase-8 (Beyotime, no: AC056), caspase-9 (Beyotime, no: AC062) and  $\beta$ -actin (Beyotime, no: AF0003) antibodies at 4 °C for overnight, followed by treatment with secondary horseradish-peroxidase-conjugated anti-rabbitIgG (Beyotime, no: A0208) for 2 h. Membranes were finally scanned in a ChemiDoc MP Imaging System (Bio-Rad) after 2 min incubation in Clarity Western ECL Substrate (Bio-Rad).

#### 4.8 EC<sub>50</sub> of PI3K $\alpha$ H1047R mutant and wide-type kinases activity

EC<sub>50</sub> values of the selected compounds against PI3K $\alpha$  H1047R mutant were determined using the HTRF assay as described in the literature [53]. Compounds were

dissolved in DMSO as stocking solution, and serially diluted in PBS to a final concentration of DMSO as 2.5%. The results were obtained using an EnSpire Multimode Plate Reader (PerkinElmer; 320/620/665) and analyzed using GraphPad Prism 6 nonlinear regression (curve fit), log (inhibitor) vs. response variable slope (four parameters) with constraints added at 0 and 100.

#### **4.9 EC<sub>50</sub> of PI3Ks kinase activity**

The assay was carried out as described previously [62]. All of the enzymatic reactions were conducted at 30°C for 40 min. First, we prepared 50 µL reaction mixtures containing 40 mM Tris (pH = 7.4), 10 mM MgCl<sub>2</sub>, 0.1 mg/mL BSA, 1 mM DTT, 0.2 µg/mL PI3Ks and 100 µM lipid substrate. Compounds were diluted in 10% DMSO, then 5 µL of the dilution with 100 µM ATP was added to the 50 µL reaction mixtures so that the final concentration of DMSO is 1% in all of reactions. The assay was then performed by using Kinase-Glo Plus luminescence kinase assay kit (Promega, no: V3771) to measure the kinase activity by quantitating the amount of ATP remaining in solution after kinase reaction. The luminescent signal is correlated with the amount of ATP remaining in the solution, and is inversely correlated with the amount of kinases activity. The EC<sub>50</sub> values were calculated using nonlinear regression with normalized dose–response fit using Prism GraphPad software.

#### **4.10 Molecular docking**

Molecular docking was performed using a Sybyl-X 2.0 software. The crystal structure of PI3K $\alpha$  H1047R mutant protein was downloaded from the Protein Data Bank (PDB ID: 3hhm). The crystal structure of PI3K $\alpha$  was optimized with H added and charge added by AMBER7 FF99 method. The structures of small molecular database were subjected to the polar H adding and being energy optimized with a tripos force field and charged optimized with Gasteiger-Huckel method.

#### **4.11 Statistical analysis**

Data are reported as means  $\pm$  SD. Statistical analysis was performed using GraphPad Prism version. \* $p < 0.05$  and \*\* $p < 0.01$  were considered as statistically significant.

## Acknowledgments

We thank the financial support from National Natural Science Foundation of China (No. 21572027 to YH), the Ministry of Science and Technology of China (2014DFG32200 to M-WW), Shanghai Science and Technology Development Fund (15DZ2291600 to M-WW) and the Thousand Talents Program in China (to YH and M-WW).

## References

- [1] K.D. Courtney, R.B. Corcoran, J.A. Engelman, The PI3K pathway as drug target in human cancer, *J. Clin. Oncol.* 28 (2010) 1075–1083.
- [2] T.M. Bauer, M.R. Patel, J.R. Infante, Targeting PI3 kinase in cancer, *Pharmacol. Ther.* 146 (2015) 53–60.
- [3] P. Xia, X.-Y. Xu, PI3K/Akt/mTOR signaling pathway in cancer stem cells: from basic research to clinical application, *Am. J. Cancer Res.* 5 (2015) 1602–1609.
- [4] V. Asati, D.K. Mahapatra, S.K. Bharti, PI3K/Akt/mTOR and Ras/Raf/MEK/ERK signaling pathways inhibitors as anticancer agents: Structural and pharmacological perspectives, *Eur. J. Med. Chem.* 109 (2016) 314–341.
- [5] J.A. Engelman, Targeting PI3K signalling in cancer: opportunities, challenges and limitations, *Nat. Rev. Cancer* 9 (2009) 550–562.
- [6] B. Vanhaesebroeck, J. Guillermet-Guibert, M. Graupera, B. Bilanges, The emerging mechanisms of isoform-specific PI3K signalling, *Nat. Rev. Mol. Cell Bio.* 11 (2010) 329–341.
- [7] R. Dienstmann, J. Rodon, V. Serra, J. Tabernero, Picking the point of inhibition: a comparative review of PI3K/AKT/mTOR pathway inhibitors, *Mol. Cancer Ther.* 13 (2014) 1021–1031.
- [8] F.I. Raynaud, S. Eccles, P.A. Clarke, A. Hayes, B. Nutley, S. Alix, A. Henley, F. Di-Stefano, Z. Ahmad, S. Guillard, L.M. Bjerke, L. Kelland, M. Valenti, L. Patterson, S. Gowan, A.d.H. Brandon, M. Hayakawa, H. Kaizawa, T. Koizumi, T. Ohishi, S. Patel, N. Saghir, P. Parker, M. Waterfield, P. Workman, Pharmacologic characterization of a potent inhibitor of class I phosphatidylinositide 3-kinases, *Cancer Res.* 67 (2007) 5840–5850.
- [9] P. Workman, P.A. Clarke, F.I. Raynaud, R.L.M. van Montfort, Drugging the PI3

kinome: from chemical tools to drugs in the clinic, *Cancer Res.*, 70 (2010) 2146–2157.

[10] L.M. Thorpe, H. Yuzugullu, J.J. Zhao, PI3K in cancer: divergent roles of isoforms, modes of activation and therapeutic targeting, *Nat. Rev. Cancer* 15 (2015) 7–24.

[11] T.W. Miller, B.N. Rexer, J.T. Garrett, C.L. Arteaga, Mutations in the phosphatidylinositol 3-kinase pathway: role in tumor progression and therapeutic implications in breast cancer, *Breast Cancer Res.* 13 (2011). 224–235.

[12] L.W.T. Cheung, B.T. Hennessy, J. Li, S. Yu, A.P. Myers, B. Djordjevic, Y. Lu, K. Stemke-Hale, M.D. Dyer, F. Zhang, Z. Ju, L.C. Cantley, S.E. Scherer, H. Liang, K.H. Lu, R.R. Broaddus, G.B. Mills, High frequency of PIK3R1 and PIK3R2 mutations in endometrial cancer elucidates a novel mechanism for regulation of PTEN protein stability, *Cancer Discov.* 1 (2011) 170–185.

[13] C. Massacesi, E. Di Tomaso, P. Urban, C. Germa, C. Quadt, L. Trandafir, P. Aimone, N. Fretault, B. Dharan, R. Tavorath, S. Hirawat, PI3K inhibitors as new cancer therapeutics: implications for clinical trial design, *OncoTargets Ther.* 9 (2016) 203–210.

[14] A.G. Bader, S.Y. Kang, P.K. Vogt, Cancer-specific mutations in PIK3CA are oncogenic in vivo, *Proc. Natl. Acad. Sci. U. S. A.* 103 (2006) 1475–1479.

[15] H. Yamamoto, H. Shigematsu, M. Nomura, W.W. Lockwood, M. Sato, N. Okumura, J. Soh, M. Suzuki, I.I. Wistuba, K.M. Fong, H. Lee, S. Toyooka, H. Date, W.L. Lam, J.D. Minna, A.F. Gazdar, PIK3CA mutations and copy number gains in human lung cancers, *Cancer Res.* 68 (2008) 6913–6921.

[16] S. Ogino, K. Nosho, G.J. Kirkner, K. Shima, N. Irahara, S. Kure, A.T. Chan, J.A. Engelman, P. Kraft, L.C. Cantley, E.L. Giovannucci, C.S. Fuchs, PIK3CA mutation is associated with poor prognosis among patients with curatively resected colon cancer, *J. Clin. Oncol.* 27 (2009) 1477–1484.

[17] X. Liao, T. Morikawa, P. Lochhead, Y. Imamura, A. Kuchiba, M. Yamauchi, K. Nosho, Z.R. Qian, R. Nishihara, J.A. Meyerhardt, C.S. Fuchs, S. Ogino, Prognostic role of PIK3CA mutation in colorectal cancer: cohort study and literature review, *Clin. Cancer Res.* 18 (2012) 2257–2268.

[18] S. Loibl, G. von Minckwitz, A. Schneeweiss, S. Paepke, A. Lehmann, M. Rezai,

D.M. Zahm, P. Sinn, F. Khandan, H. Eidtmann, K. Dohnal, C. Heinrichs, J. Huober, B. Pfitzner, P.A. Fasching, F. Andre, J.L. Lindner, C. Sotiriou, A. Dykgers, S. Guo, S. Gade, V. Nekljudova, S. Loi, M. Untch, C. Denkert, PIK3CA mutations are associated with lower rates of pathologic complete response to anti-human epidermal growth factor receptor 2 (HER2) therapy in primary HER2-overexpressing breast cancer, *J. Clin. Oncol.* 32 (2014) 3212–3220.

[19] M.J. Higgins, D. Jelovac, E. Barnathan, B. Blair, S. Slater, P. Powers, J. Zorzi, S.C. Jeter, G.R. Oliver, J. Fetting, L. Emens, C. Riley, V. Stearns, F. Diehl, P. Angenendt, P. Huang, L. Cope, P. Argani, K.M. Murphy, K.E. Bachman, J. Greshock, A.C. Wolff, B.H. Park, Detection of tumor PIK3CA status in metastatic breast cancer using peripheral blood, *Clin. Cancer Res.* 18 (2012) 3462–3469.

[20] K. Kalinsky, L.M. Jacks, A. Heguy, S. Patil, M. Drobnjak, U.K. Bhanot, C.V. Hedvat, T.A. Traina, D. Solit, W. Gerald, M.E. Moynahan, PIK3CA mutation associates with improved outcome in breast cancer, *Clin. Cancer Res.* 15 (2009) 5049–5059.

[21] O. Kawano, H. Sasaki, K. Endo, E. Suzuki, H. Haneda, H. Yukiue, Y. Kobayashi, M. Yano, Y. Fujii, PIK3CA mutation status in Japanese lung cancer patients, *Lung Cancer* 54 (2006) 209–215.

[22] C.-H. Huang, D. Mandelker, O. Schmidt-Kittler, Y. Samuels, V.E. Velculescu, K.W. Kinzler, B. Vogelstein, S.B. Gabelli, L.M. Amzel, The structure of a human p110 alpha/p85 alpha complex elucidates the effects of oncogenic PI3K alpha mutations, *Science* 318 (2007) 1744–1748.

[23] G. Cathomas, PIK3CA in colorectal cancer, *Front. Oncol.* 4 (2014) 35–35.

[24] D.T. Kumar, C.G.P. Doss, Role of E542 and E545 missense mutations of PIK3CA in breast cancer: a comparative computational approach, *J. Biomol. Struct. Dyn.* 35 (2017) 2745–2757.

[25] T.K.H. Chung, T.H. Cheung, S.F. Yim, M.Y. Yu, R.W.K. Chiu, K.W.K. Lo, I.P.C. Lee, R.R.Y. Wong, K.K.M. Lau, V.W. Wang, M.J. Worley, Jr., K.M. Elias, S.J. Fiascone, D.I. Smith, R.S. Berkowitz, Y.F. Wong, Liquid biopsy of PIK3CA mutations in cervical cancer in Hong Kong Chinese women, *Gynecol. Oncol.* 146 (2017) 334–339.

[26] S.T. Kim, M. Lira, S. Deng, S. Lee, Y.S. Park, H.Y. Lim, W.K. Kang, M. Mao, J.S. Heo, W. Kwon, K.-T. Jang, J. Lee, J.O. Park, PIK3CA mutation detection in

- metastatic biliary cancer using cell-free DNA, *Oncotarget* 6 (2015) 40026–40035.
- [27] F. Janku, J.J. Wheler, A. Naing, G.S. Falchook, D.S. Hong, V.M. Stepanek, S. Fu, S.A. Piha-Paul, J.J. Lee, R. Luthra, A.M. Tsimberidou, R. Kurzrock, PIK3CA mutation H1047R is associated with response to PI3K/AKT/mTOR signaling pathway inhibitors in early-phase clinical trials, *Cancer Res.* 73 (2013) 276–284.
- [28] M.S. Miller, O. Schmidt-Kittler, D.M. Bolduc, E.T. Brower, D. Chaves-Moreira, M. Allaire, K.W. Kinzler, I.G. Jennings, P.E. Thompson, P.A. Cole, L.M. Amzel, B. Vogelstein, S.B. Gabelli, Structural basis of nSH2 regulation and lipid binding in PI3K alpha, *Oncotarget* 5 (2014) 5198–5208.
- [29] C. Hafner, E. Lopez-Knowles, N.M. Luis, A. Toll, E. Baselga, A. Fernandez-Casado, S. Hernandez, A. Ribe, T. Mentzel, R. Stoehr, F. Hofstaedter, M. Landthaler, T. Vogt, R.M. Pujol, A. Hartmann, F.X. Real, Oncogenic PIK3CA mutations occur in epidermal nevi and seborrheic keratoses with a mutation pattern, *Proc. Natl. Acad. Sci. U. S. A.* 104 (2007) 13450–13454.
- [30] L. Zhao, P.K. Vogt, Helical domain and kinase domain mutations in p110 alpha of phosphatidylinositol 3-kinase induce gain of function by different mechanisms, *Proc. Natl. Acad. Sci. U. S. A.* 105 (2008) 2652–2657.
- [31] M. Barbareschi, F. Buttitta, L. Felicioni, S. Cotrupi, F. Barassi, M. Del Grammastro, A. Ferro, P.D. Palma, E. Galligioni, A. Marchetti, Different prognostic roles of mutations in the helical and kinase domains of the PIK3CA gene in breast carcinomas, *Clin. Cancer Res.* 13 (2007) 6064–6069.
- [32] F. Schonleben, W.L. Qiu, N.T. Ciau, D.J. Ho, X.J. Li, J.D. Allendorf, H.E. Remotti, G.H. Su, PIK3CA mutations in intraductal papillary mucinous neoplasm/carcinoma of the pancreas, *Clin. Cancer Res.* 12 (2006) 3851–3855.
- [33] J.E. Burke, O. Perisic, G.R. Masson, O. Vadas, R.L. Williams, Oncogenic mutations mimic and enhance dynamic events in the natural activation of phosphoinositide 3-kinase p110 alpha (PIK3CA), *Proc. Natl. Acad. Sci. U. S. A.* 109 (2012) 15259–15264.
- [34] F. Janku, D.S. Hong, S. Fu, S.A. Piha-Paul, A. Naing, G.S. Falchook, A.M. Tsimberidou, V.M. Stepanek, S.L. Moulder, J.J. Lee, R. Luthra, R.G. Zinner, R.R. Broaddus, J.J. Wheler, R. Kurzrock, Assessing PIK3CA and PTEN in early-phase trials with PI3K/AKT/mTOR inhibitors, *Cell Reports* 6 (2014) 377–387.

- [35] S. Jamieson, J.U. Flanagan, S. Kolekar, C. Buchanan, J.D. Kendall, W.-J. Lee, G.W. Rewcastle, W.A. Denny, R. Singh, J. Dickson, B.C. Baguley, P.R. Shepherd, A drug targeting only p110 alpha can block phosphoinositide 3-kinase signalling and tumour growth in certain cell types, *Biochem. J* 438 (2011) 53–62.
- [36] J.D. Carson, G. Van Aller, R. Lehr, R.H. Sinnamon, R.B. Kirkpatrick, K.R. Auger, D. Dhanak, R.A. Copeland, R.R. Gontarek, P.J. Tummino, L. Luo, Effects of oncogenic p110 alpha subunit mutations on the lipid kinase activity of phosphoinositide 3-kinase, *Biochem. J* 409 (2008) 519–524.
- [37] J.A. Engelman, L. Chen, X. Tan, K. Crosby, A.R. Guimaraes, R. Upadhyay, M. Maira, K. McNamara, S.A. Perera, Y. Song, L.R. Chirieac, R. Kaur, A. Lightbown, J. Simendinger, T. Li, R.F. Padera, C. Garcia-Echeverria, R. Weissleder, U. Mahmood, L.C. Cantley, K.-K. Wong, Effective use of PI3K and MEK inhibitors to treat mutant Kras G12D and PIK3CA H1047R murine lung cancers, *Nat. Med.* 14 (2008) 1351–1356.
- [38] V. Serra, B. Markman, M. Scaltriti, P.J.A. Eichhorn, V. Valero, M. Guzman, M. Luisa Botero, E. Llonch, F. Atzori, S. Di Cosimo, M. Maira, C. Garcia-Echeverria, J. Lluís Parra, J. Arribas, J. Baselga, NVP-BEZ235, a dual PI3K/mTOR inhibitor, prevents PI3K signaling and inhibits the growth of cancer cells with activating PI3K mutations, *Cancer Res.* 68 (2008) 8022–8030.
- [39] J. Rodon, R. Dienstmann, V. Serra, J. Tabernero, Development of PI3K inhibitors: lessons learned from early clinical trials, *Nat. Rev. Clin. Oncol.* 10 (2013) 143–153.
- [40] F. Janku, A.M. Tsimberidou, I. Garrido-Laguna, X. Wang, R. Luthra, D.S. Hong, A. Naing, G.S. Falchook, J.W. Moroney, S.A. Piha-Paul, J.J. Wheler, S.L. Moulder, S. Fu, R. Kurzrock, PIK3CA mutations in patients with advanced cancers treated with PI3K/AKT/mTOR axis inhibitors, *Mol. Cancer Ther.* 10 (2011) 558–565.
- [41] J. Rodon, I. Brana, L.L. Siu, M.J. De Jonge, N. Homji, D. Mills, E. Di Tomaso, C. Sarr, L. Trandafir, C. Massacesi, F. Eskens, J.C. Bendell, Phase I dose-escalation and expansion study of buparlisib (BKM120), an oral pan-Class I PI3K inhibitor, in patients with advanced solid tumors, *Invest. New Drugs* 32 (2014) 670–681.
- [42] J.C. Bendell, J. Rodon, H.A. Burris, M. de Jonge, J. Verweij, D. Birle, D. Demanase, S.S. De Buck, Q.C. Ru, M. Peters, M. Goldbrunner, J. Baselga, Phase I, Dose-escalation study of BKM120, an oral Pan-class I PI3K inhibitor, in patients with advanced solid tumors, *J. Clin. Oncol.* 30 (2012) 282–290.

- [43] S.-M. Maira, S. Pecchi, A. Huang, M. Burger, M. Knapp, D. Sterker, C. Schnell, D. Guthy, T. Nagel, M. Wiesmann, S. Brachmann, C. Fritsch, M. Dorsch, P. Chene, K. Shoemaker, A. De Pover, D. Menezes, G. Martiny-Baron, D. Fabbro, C.J. Wilson, R. Schlegel, F. Hofmann, C. Garcia-Echeverria, W.R. Sellers, C.F. Voliva, Identification and characterization of NVP-BKM120, an orally available Pan-Class I PI3-kinase inhibitor, *Mol. Cancer Ther.* 11 (2012) 317–328.
- [44] C.X. Ma, J. Luo, M. Naughton, F. Ademuyiwa, R. Suresh, M. Griffith, O.L. Griffith, Z.L. Skidmore, N.C. Spies, A. Ramu, L. Trani, T. Pluard, G. Nagaraj, S. Thomas, Z. Guo, J. Hoog, J. Han, E. Mardis, C. Lockhart, M.J. Ellis, A phase I trial of BKM120 (Buparlisib) in combination with fulvestrant in postmenopausal women with estrogen receptor-positive metastatic breast cancer, *Clin. Cancer Res.* 22 (2016) 1583–1591.
- [45] I.A. Mayer, V.G. Abramson, L. Formisano, J.M. Balko, M.V. Estrada, M.E. Sanders, D. Juric, D. Solit, M.F. Berger, H.H. Won, Y. Li, L.C. Cantley, E. Winer, C.L. Arteaga, A phase Ib study of Alpelisib (BYL719), a PI3K alpha-specific inhibitor, with letrozole in ER<sup>+</sup>/HER2(-) metastatic breast cancer, *Clin. Cancer Res.* 23 (2017) 26–34.
- [46] A. James, L. Blumenstein, U. Glaenzel, Y. Jin, A. Demailly, A. Jakab, R. Hansen, K. Hazell, A. Mehta, L. Trandafir, P. Swart, Absorption, distribution, metabolism, and excretion of C-14 BYL719 (alpelisib) in healthy male volunteers, *Cancer Chemother. Pharmacol.* 76 (2015) 751–760.
- [47] I.C. Chen, L.-P. Hsiao, I.W. Huang, H.-C. Yu, L.-C. Yeh, C.-H. Lin, T.W.-W. Chen, A.-L. Cheng, Y.-S. Lu, Phosphatidylinositol-3 kinase inhibitors, Buparlisib and Alpelisib, sensitize estrogen receptorpositive breast cancer cells to tamoxifen, *Sci. Rep.* 7 (2017) 9842.
- [48] K. Masui, B. Gini, J. Wykosky, C. Zanca, P.S. Mischel, F.B. Furnari, W.K. Cavenee, A tale of two approaches: complementary mechanisms of cytotoxic and targeted therapy resistance may inform next-generation cancer treatments, *Carcinogenesis* 34 (2013) 725–738.
- [49] J.A. Beaver, D. Jelovac, S. Balukrishna, R.L. Cochran, S. Croessmann, D.J. Zabransky, H.Y. Wong, P.V. Toro, J. Cidado, B.G. Blair, D. Chu, T. Burns, M.J. Higgins, V. Stearns, L. Jacobs, M. Habibi, J. Lange, P.J. Hurley, J. Lauring, D.A. VanDenBerg, J. Kessler, S. Jeter, M.L. Samuels, D. Maar, L. Cope, A.

- Cimino-Mathews, P. Argani, A.C. Wolff, B.H. Park, Detection of cancer DNA in plasma of patients with early-stage breast cancer, *Clin. Cancer Res.* 20 (2014) 2643–2650.
- [50] G. Ligresti, L. Militello, L.S. Steelman, A. Cavallaro, F. Basile, F. Nicoletti, F. Stivala, J.A. McCubrey, M. Libra, PIK3CA mutations in human solid tumors role in sensitivity to various therapeutic approaches, *Cell Cycle* 8 (2009) 1352–1358.
- [51] P. Gkeka, T. Evangelidis, M. Pavlaki, V. Lazani, S. Christoforidis, B. Agianian, Z. Cournia, Investigating the structure and dynamics of the PIK3CA wild-type and H1047R oncogenic mutant, *PLoS Comput. Biol.* 10 (2014) e1003895.
- [52] J.P. Gustin, D.P. Cosgrove, B.H. Park, The PIK3CA gene as a mutated target for cancer therapy, *Curr. Cancer Drug Tar.* 8 (2008) 733–740.
- [53] J. Wang, G.Q Gong, Y. Zhou, W.J Lee, C. M Buchanan, W. A Denny, G.W Rewcastle, J. D Kendall, M.J Dickson, J.U Flanagan, P. R. Shepherd, D.H. Yang and M.W Wang. High-throughput screening campaigns against PI3K $\alpha$  isoform bearing the H1047R mutation identified potential inhibitors with novel scaffolds. *Acta Pharmacol. Sin.* (2018) DOI: 10.1038/s41401-018-0057-z.
- [54] H. Zang, E.Y.X. Chen, Organocatalytic upgrading of furfural and 5-hydroxymethyl furfural to C-10 and C-12 furoins with quantitative yield and atom-efficiency, *Int. J. Mol. Sci.* 16 (2015) 7143–7158.
- [55] H.M. Bachhav, S.B. Bhagat, V.N. Telvekar, Efficient protocol for the synthesis of quinoxaline, benzoxazole and benzimidazole derivatives using glycerol as green solvent, *Tetrahedron Lett.* 52 (2011) 5697–5701.
- [56] A. Kamal, K.S. Babu, S.M.A. Hussaini, R. Mahesh, A. Alarifi, Amberlite IR-120H, an efficient and recyclable solid phase catalyst for the synthesis of quinoxalines: a greener approach, *Tetrahedron Lett.* 56 (2015) 2803–2808.
- [57] K.B. Harsha, K.S. Rangappa, One-step approach for the synthesis of functionalized quinoxalines mediated by T3P (R)-DMSO or T3P (R) via a tandem oxidation-condensation or condensation reaction, *RSC Adv.* 6 (2016) 57154–57162.
- [58] A. Kamal, K.S. Babu, S. Faazil, S.M.A. Hussaini, A.B. Shaik, L-Proline mediated synthesis of quinoxalines; evaluation of cytotoxic and antimicrobial activity, *Rsc Adv.* 4 (2014) 46369–46377.
- [59] A. Go, G. Lee, J. Kim, S. Bae, B.M. Lee, B.H. Kim, One-pot synthesis of quinoxalines from reductive coupling of 2-nitroanilines and 1,2-diketones using

indium, *Tetrahedron* 71 (2015) 1215–1226.

[60] Z. Zhang, C. Xie, L. Feng, C. Ma, PTSA-catalyzed one-pot synthesis of quinoxalines using DMSO as the oxidant, *Synthetic Commun.*, 46 (2016) 1507–1518.

[61] D.E. Ames, M.I. Brohi, Alkynyl-quinoxalines and dialkynyl-quinoxalines-synthesis of condensed quinoxalines, *J. Chem. Soc. Perkin. Trans. 1* (1980) 1384–1389.

[62] M.A. Kashem, R.M. Nelson, J.D. Yingling, S.S. Pullen, A.S.P. III, J.W. Jones, J.P. Wolak, G.R. Rogers, M.M. Morelock, R.J. Snow, C.A. Homon, S. Jakes, Three mechanistically distinct kinase assays compared: Measurement of intrinsic ATPase activity identified the most comprehensive set of ITK inhibitors, *J. Biomol. Screen.* 12 (2007) 70–83.

**Highlights**

- ▶ Compound **7b** displayed a potent PI3K $\alpha$  H1047R inhibitory activity
- ▶ Compound **7b** strongly inhibited HCT116 cancer cell proliferation
- ▶ Compound **7b** had little effect on other PI3K isoforms